

## Research

# Advanced AuNMs as Nanomedicine's central Goals Capable of Active Targeting in Both Imaging and Therapy in Biomolecules

Loutfy H Madkour\*

*Chemistry Department, Faculty of Science and Arts, Baljarashi, Al Baha University, Baljarashi 65635, Saudi Arabia*

## Abstract

The stability and dispersity of AuNMs in solution play a key role for the many applications. Most inorganic nonmaterial's are not well dispersed in physiological buffers and require functionalization by thiols or surfactants to offer the stabilization forces. Furthermore, sufficient blood circulation time is critical for both imaging and in *vivo* drug delivery. Localized surface Plasmon resonance (LSPR) is one of the most significant features of AuNMs. The AuNMs as reporters have been broadly applied into lateral flow immunochromatographical assay (LFICA) and enzyme-linked immunosorbent assay (ELISA), which is a well-established technology for analysis of the target analytes in food safety, clinical diagnosis, environmental monitoring, and medical science and soon. Au based nonmaterial's (AuNMs) are known to possess many attractive features such as unique electrical, optical and catalytic properties as well as excellent biocompatibility. In this review, we summarize the current advancement on application of AuNMs in analytical sciences based on their local surface Plasmon resonance, fluorescence and electrochemistry properties. AuNMs based imaging and therapy in biomolecular is explained. As one of the most reliable imaging modes, computed tomography (CT), X-ray and SERS imaging has been widely used owing to its high spatial and density resolution. We end the review by a discussion of the conjugation between gold nanoparticles with other kinds of nanoparticles such as other metals and carbon nanostructures. Finally, future development in this research area is also prospected.

## Introduction

In 2017 Madkour, L.H. [1] presents a vision for life sciences: through interfaces between nanoelectronic and biological systems in order to the prevention and treatment of disease in the human body. In this article, we review the applications of gold nanoparticles in medicine. Generally, the recognition elements, which are applied into colorimetric sensors based on AuNMs, are categorized as follows: (1) antibodies or proteins modified AuNMs with immuno reaction, (2) chemically-modified AuNMs with non-covalent bond recognition, and (3) aptamers modified AuNMs with conformational change. Furthermore, some novel techniques

have been tried to improve the selectivity of colorimetric sensing, such as click-chemistry-based assay.

Physics, chemistry and biology of Au based nonmaterial's (AuNMs) have emerged as a broad and new sub discipline in the community of colloids and surfaces. The specific size and shape dependent physiochemical properties and remarkable bio/chemical inertness of AuNMs have

made themselves the ideal candidates for both fundamental and technical study including crystal growth, electron-transfer mechanism, localized electro-magnetic theory, catalysis, DNA assay, bioimaging and therapy, and so on [2]. Among those rich properties, the optical characteristics originated from the giant electromagnetic field near the surface of AuNMs are particularly intriguing and thus broadly applied in analytical science, e.g. colorimetric assay, surface enhanced Raman spectroscopy (SERS) and surface Plasmon resonance (SPR) spectroscopy, as well as bioimaging. Another interesting optical property of AuNMs is that fluorescence appears with their size shrinkage to below 2 nm, which allows development of luminescence-based analysis. Also, electrochemical (EC) sensors could be constructed based on the redox feature of Au NMs (Figure 1). Analytical science has been playing a primary role in our daily life, for instance, food safety control [3], biomedical diagnosis [4], medico legal appraisalment [5], anti-terrorism alert [6], and environmental pollution

**\*Corresponding author:** Loutfy H Madkour, Chemistry Department, Faculty of Science and Arts, Baljarashi, Al Baha University, Baljarashi 65635, Saudi Arabia, Tel; +966 533899075; Fax: +966 77247272; E-mail: loutfy\_madkour@yahoo.com / lha.madkour@gmail.com / Lmadkour@bu.edu.sa

**Sub Date:** April 13, 2017, **Acc Date:** May 3, 2017, **Pub Date:** May 3, 2017.

**Citation:** Loutfy H Madkour (2017) Advanced AuNMs as Nanomedicine's central Goals Capable of Active Targeting in Both Imaging and Therapy in Biomolecules. BAOJ Nanotech 3: 015.

**Copyright:** © 2017 Loutfy H Madkour. This is an open-access article distributed under the terms of the Creative Commons Attribution License, which permits unrestricted use, distribution, and reproduction in any medium, provided the original author and source are credited.

monitoring [7]. Efficient detection technologies depend greatly on the analytical method in terms of analysis time, signal-to-noise (S/N) ratio, selectivity, and limit of detection (LOD) [8]. Therefore, a great of efforts should be paid to develop new analytical methods with the advantages of rapid determination, high analysis flux, satisfactory sensitivity and good robustness. Thanks to the above-mentioned optical and electrochemical features, many functionalized AuNMs have been successfully synthesized [9–14] for improving performances of analytical techniques.



Fig. 1. Application of AuNMs in analytical science.

### Small Organic Molecules and Metal Ions

For the sensitive detection of small organic molecules, the AuNMs play an important role in improving sensitivity of the EC sensors. Especially, AuNMs composited with conducting polymers or carbon nonmaterial's have been used to increase electro-chemical efficiency. It deserves noting that the decorated carbon nanomaterials with metal NPs are of special interest due to the integrated property of two components with better catalytic activity and enhanced electrical conductivity [15,16]. Zhu et al. fabricated EC sensors by using spherical AuNPs combined with conducting polymer (poly-[2, 5-di-(2- thienyl)-1H-pyrrole-1-(p-benzoicacid)]) [17]. To further improve electron transfer, synergistic effect of multiple nanocomposite layers, namely, chitosan-AuNPs, graphene-AuNPs and multi-walled carbon nanotubes (MWCNTs)-cobalt phthalocyanine, was exploited by Sun et al. [18]. Roushaniet al. [19] fabricated a sensitive and selective EC apta sensor for detection of cocaine based on the conformational change of the aptamer-functionalized AuNPs onto CNTs-based nanocomposite.

Detection of organic small molecules and metal ions is very important for controlling food quality, environmental protection

and antiterrorism. In order to realize detection of trace amount of analytes at extremely low concentrations, various efforts for increasing the sensitivity of SPR biosensors have been paid. Most of these methods are based on changing the refractive index at the sensor surfaces by means of a variety of (bio) chemical or NP agents, which are captured by the sensor surfaces subsequent to the binding of the target analyte to the primary biorecognition elements. These methods include the use of secondary and tertiary antibodies, antibodies labeled with enzymes, and dielectric or metallic NPs [20]. In particular, AuNMs of diameters ranging from 5 to 40 nm have been widely used to enhance the response of SPR biosensors [21,22].

### Metal Ions

Some EC sensor methods based on AuNMs have been developed for detection of heavy metal ions. For examples, Shen et al.[23] proposed an EC DNAzyme sensor based on AuNPs for sensitive and selective detection of  $Pb^{2+}$ . A label-free EC sensor was developed for the highly sensitive and selective detection of  $Hg^{2+}$  by Tang et al [24]. In their study, the catalytic  $H AuCl_4 / NH_2 OH$  reaction was utilized for formation of AuNPs as signal reporter after capturing  $Hg^{2+}$  on the modified electrode surface through the specific thymine- $Hg^{2+}$ -thymine (T- $Hg^{2+}$ -T) coordination. Compared with the traditional metal NPs-based method, this sensor avoided the labeling of the DNA probe with NP tags, and only one unlabeled T-rich DNA sequence was needed, which greatly reduced the cost and simplified the sensing procedure. Thus, a LOD as low as 0.06 nM could be obtained for  $Hg^{2+}$ . Furthermore, in 2016, Wang et al. presented a sensitive, selective and reusable EC biosensor for determination of  $Hg^{2+}$  based on thymine modified AuNPs/reduced graphene oxide nanocomposites [25] (Fig. 2). Notably, the developed EC sensors afforded excellent selectivity for  $Hg^{2+}$  against other heavy metal ions including  $Zn^{2+}$ ,  $Cd^{2+}$ ,  $Pb^{2+}$ ,  $Cu^{2+}$ ,  $Ni^{2+}$  and  $Co^{2+}$ . Wang et al. prepared an EC sensor based on graphene and AuNPs for detection of trace  $Cu^{2+}$  with the anodic stripping voltammeter analysis [26]. Yang et al. constructed a highly sensitive electro-chemical DNA biosensor made of polyaniline (PANI) and AuNPs nanocomposite (AuNPs@PANI) for detection of trace concentration of  $Ag^+$  [27]. In the presence of  $Ag^+$ , with interaction of cytosine- $Ag^+$ -cytosine (C- $Ag^+$ -C), cytosine-rich DNA sequence immobilized onto the surface of AuNPs@PANI had a self-hybridization and then formed a duplex-like structure. The prepared EC sensors could detect  $Ag^+$  at a wide linear range of 0.01–100 nM with a LOD of 10 pM.

### Synthesis of AuNMs

Traditionally, the tri-sodium citrate-based thermal reduction has been broadly recognized as a universal approach for preparing spherical Au nanoparticles (AuNPs) of varied sizes ranging from 15 to 147 nm possessing strong SPR signals [28]. Although



Fig. 2. Scheme of thymidine functionalized biosensor for  $Hg^{2+}$  detection. Printed with permission from [25]. Copyright 2016 Elsevier.

this preparation method simply involves controlling the ratios of citrate to Au ions [29], the reaction often needs to be carried out on a relatively large scale at the temperature of boiling water and lacks the reproducible preparation of uniform AuNPs with rather large sizes. After the breakthroughs reported by Schmid [30, 31] and Brust et al. [32], a variety of methods have been developed to synthesize AuNMs, and many excellent reviews [33] are available now. In general, the reported synthesis methods of spherical AuNMs can be categorized as followed: (1) citrate reduction; (2) Brust-Schiffrin phase transfer synthesis; (3) other sulfur-containing ligands method; (4) soft templates including micro emulsion, reversed Micelles, surfactants, membranes and polyelectrolyte's; (5) seed-mediated growth; and (6) physical methods [34]. In addition, non-spherical nanoparticles (NPs) such as Au nanorods (AuNRs) [35], Au nanocages [36], Aucubes [37], Au triangular prisms [38], as well as other unconventional structures like hollow tubes and even branched nanocrystals [39] have attracted significant research attention in the past two decades, since the properties of AuNMs are known to be strongly dependent on the size and shape of the particle [40]. Recently, a lot of excellent reviews have summarized how to achieve shape- and size-defined AuNMs with different techniques including solve thermal synthesis, seed-mediated growth, homogeneous nucleation and electrochemical method [41,42]. In this review, we mainly introduce the latest and important advancement of synthesis of the AuNMs, especially on how to control the morphology of AuNMs. A great of efforts have been paid to achieve high-quality and shape-controlled AuNMs for the purpose of highly-sensitive analysis. Unfortunately, most of the synthetic methods are empirical, and understanding their growth mechanism remains a challenging task. Interestingly, introduction of  $Ag^+$  in growth solutions significantly improves the yield of AuNRs, and Yang et al. prepared AuNRs with controlled aspect ratio by using photochemistry in the presence of  $Ag^+$  [43]. This process itself was highly promising for producing uniform AuNRs, and more importantly it was useful in deciphering the growth mechanism of anisotropic AuNPs due to its simplicity and the relatively slow growth rate of the AuNRs. Later, a versatile seed-mediated growth method was reported for

selective synthesis of single crystalline rhombic dodecahedral, octahedral, and cubic AuNMs [44]. These results might provide basis for gaining mechanistic insight into the growth of shape- and structure-controlled noble metal nonmaterial. An even more complex sample is nanostar, which is characteristic of uneven arms with different lengths. To fully implement the advantageous property of Au nanostars, a precise control over their symmetry and uniformity is highly desired. In 2015, Niu et al. obtained Au nanostars with excellent symmetry control by using a solution-phase method in high yield and good monodispersity [45]. In their study, icosahedral seeds were used to dictate the growth of the evenly distributed arms in an  $I_h$  symmetric manner. Benefiting from their high symmetry, the Au nanostars exhibited much better single-particle SERS performance compared with asymmetric Au nanostars, in terms of both intensity and reproducibility. Apart from large-sized Au particles, Au nanoclusters (AuNCs) with the sizes of less than 2 nm formed in dendrimers displays visible luminescence of high quantum yield (QY) [46]. Ying et al. reported a simple, one-pot and "green" synthetic route, based on the reduction and stabilization capability of bovine serum albumin (BSA) proteins. The AuNCs prepared at the physiological temperature (37°C) showed red emission with a QY of ~6% [47]. In order to further control the luminescence property, synthesis of atomically precise AuNCs has ignited numerous research efforts [48,49]. In 2014, Yu et al. [50] synthesized  $Au_{22}(\text{glutathione})_{18}$  clusters of the emission peak at ~665 nm with a QY of ~8%. Upon comparison of their luminescence properties with those of Au(I)-thiolate complexes, the enhanced luminescence of  $Au_{22}(\text{SG})_{18}$  was ascribed to aggregation-induced emission. Nevertheless, the origin of emission in AuNCs still keeps unclear, posing a major hurdle for development of highly luminescent clusters. In 2015, Pyo et al. prepared  $Au_{22}(\text{glutathione})_{18}$  clusters with a luminescence QY greater than 60% by rigidifying their Au shell with tetraoctylammonium cations [51]. This study presents an effective strategy to enhance the luminescence efficiencies of AuNCs by optimizing the shell structure.

In order to precisely tune the size and shape of AuNMs, DNA is recently adopted as a powerful programmable tool to realize

above goals. Lu's group systematically summarized morphology controlling, spatial positioning and dynamic assembly of AuNMs with DNA as a powerful tool [52]. In some details, their research results demonstrated that DNA could be used to control the morphologies of AuNMs during seed-mediated growth [53]. They also developed a novel method based on DNA-encoded tuning to achieve AuNMs from AuNR seeds with controlled geometric and plasmonic properties [54]. Furthermore, they suggested that the DNA molecules played important roles via influencing diffusion of the Au precursors to the seed, and therefore the AuNMs growth might be modulated through difference in DNA desorption, density and mobility on the seed surfaces [55]. These insights into the mechanism of DNA-guided AuNMs synthesis not only provide deep understanding of the interactions between the DNA and nonmaterial but also allow better control of the shapes and surface properties of many nonmaterial. Ye et al. designed a millifluidic reactor to synthesize a wide variety of AuNMs at high concentrations [56]. The synthesized method based on millifluidic reactors inspired other researchers to use the analogous reactors for possible mechanism and application study. Recently, Krishna et al. demonstrated adoption of a simple millifluidic chip for in sit analysis of morphology- and dimension-controlled growth of Au nano- and micro-structures with a time resolution of 5 ms [57] (Figure 3). See from Fig. 3, gold structures with  $\sim 3 \mu\text{m}$  in diameter that had corrugated metal-like shapes were formed after a time interval of 5 h (Figure 3 d). When the time of flow was increased to 9 h, these structures further transformed into micro-hemispherical ones (Figure 3 c). This study offers a feasible way to obtain dimension-and morphology-controlled AuNMs in a high yield.

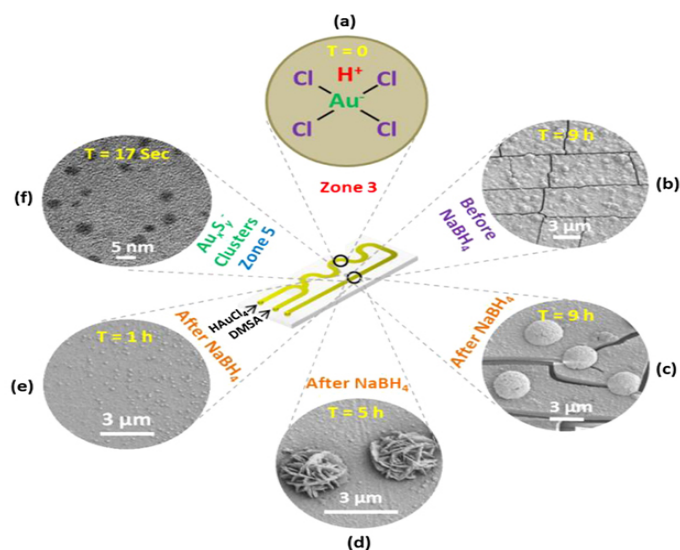


**Fig. 3.** Scheme showing different stages of spatially (and time) resolved growth process of AuNMs within millifluidic chip. Printed with permission from [57]. Copyright 2013 American Chemical Society.

Noteworthy, some novel synthesis strategies, such as biosynthesis

[58,59], 2D immiscible oil/water interface [60], levitated leidenfrost drop [61], sunlight-induced synthesis [62] and so on, have been reported, and such green and economic synthesis methods for preparation of uniform and controlled AuNMs provide the opportunity for development of low-cost and sustainable analytical techniques. However, the above technologies need to be further improved and standardized.

### Surface Modification of AuNMs

Owing to the large surface to volume ratio, modification and fictionalization of AuNMs surfaces with biomolecules, DNA or chemicals becomes imperative for their application in analytical science.

It is well known that free AuNMs have high surface energy and tend to aggregate and fuse. As a result, the intriguing properties observed for the AuNPs would disappear, and the difficulty arises for long term storage, processing, and applications. There-fore, great efforts have been devoted to develop novel strategies to stabilize AuNMs [63], and the most common approach is to coat AuNMs with either organic or inorganic shells. These shells not only endow AuNPs with high stability but also offer them additional functionalities. As an example, in addition to good stability and biocompatibility, the mesoporous silica shells that are currently broadly used have high surface area and tunable pore size and volume, which can accommodate analytes and drug molecules [64].

### Biomolecules (DNA, protein and cell)

AuNMs have been widely used in SERS based immunoassays of biomolecules such as DNA, protein and cell. However, challenges still remain with amplification of SERS signals due to the extremely small cross-section of Raman scattering [65]. Yan et al. introduced a new strategy based on nano rolling-circle amplification (nanoRCA) and nano hyper branched rolling circle amplification(nanoHRCA) to increase "hot spot" groups for protein microarrays [66]. Li et al. constructed a SERS immune sensor for detection of biomarkers [67]. In their study, the capture antibody was immobilized on the Au triangle nanoarray chip, while the detection antibody was conjugated with the SERS probe (Au@Ramanreporter@SiO<sub>2</sub>sandwich NP). The antigen (analyte) was sandwiched between the capture antibody and the detection antibody. Under light excitation, a lot of "hot spots" were created between the Au triangles in nanoarray, and thus the developed SERS immunosensor could be used for sensitive biomarker detection. Luo et al [68]. Reported a facile immunoassay for porcine circovirus type 2 (PCV2) based on SERS using multi-branched AuNPs(mb-AuNPs) as substrates. The mb-AuNPs in the immunosensor act as Raman reporters, which were prepared via Tris base-induced reduction and subsequent reaction with *p*-mercaptobenzoic acid. The modified mb-AuNPs were covalently conjugated to the mono-

clonal antibody (McAb) against the PCV2 cap protein to form SER Simmuno nanoprobles. These were captured in a microtiterplate via an immunoreactions in the presence of target antigens. Compared to conventional detecting methods such as those based on PCR, themethod was demonstrated to be rapid, facile and very sensitive. Tang et al. developed a simple and reproducible SERS chip for highly sensitive and selective screening of active ricin in complex matrices [69]. They fabricated single strand oligodeoxynucleotides modified AuNPs in order to amplify recognition and reaction by virtue of their cooperative binding property. To improve sensitivity of this method, a Ag nano shell was deposited on post-reacted poly(21dA)-AuNPs, which lowered LOD to 8.9 ng mL<sup>-1</sup>.

The utilization of SERS-based techniques in targeting specific DNA and RNA sequences is generally realized by combination with AuNMs and Raman-active molecules [70,71]. Wang et al. raised a concept to use enzyme controlled plasmonic coupling as SERS nanosensors for DNA demethylation [72]. The nanosensors were constructed by decorating AuNPs with Raman reporters and hemi ethylated DNA probes. The enzymatic degradation of DNA substrate probes was utilized to induce aggregation of AuNPs, so the reproducible and sensitive SERS signals were achieved from biological recognition events. Development of SERS-bar-coded particles, which contain multiple Raman-active molecules and are insensitive to photo bleaching, is particularly intriguing for high-throughput and multiplex DNA screening [73]. Recently, Chenet al. prepared a SERS-bar-coded nanosensor to detect *Bacillusthuringiensis* (*Bt*) gene transformed rice expressing insecticidal proteins [74]. The bar-coded sensor was designed by encapsulation of AuNPs with silica and conjugation of oligonucleotide strands for targeting DNA strands. The transition between the *cry1A* (b) and *cry1A*(c) fusion gene sequence was used to construct a specific SERS-based detection method with a LOD of 0.1 pg/mL. In order to build the determination models to screen transgene, a series mixture of *Bt* rice and normal rice were prepared for SERS assay, and the LOD was 0.1% (w/w) was explored for transgenic *Bt* rice relative to normal rice. The sensitivity and accuracy of the SERS-based assay were comparable with real-time PCR. Recently, Ye et al. proposed an asymmetric signal amplification method for simultaneously detecting multiple biomarkers with significantly different levels [75]. The bio barcode consisted of a large number of signals DNA (Cy3-DNA for Cy3-bio barcode or Rox-DNA for Rox-bio barcode) and capture DNA immobilized onto the Au NPs. The AuNPs simultaneously act both as a Raman-signal-enhancing substrate and a Raman signal carrier. Using these bifunctional probes, a linear amplification mode was obtained with high-concentration markers, whereas quadratic amplification mode was responsible to low-concentration markers.

Detection of circulating tumor cells (CTCs) in the blood of cancer

patients is significant for early cancer diagnosis, cancer prognosis, evaluation of the treatment effect of chemotherapy drugs, and choice of cancer treatment options [76]. In 2011, Wang et al. introduced SERS technology for direct detection of target CTCs in human peripheral blood. The LOD of this method ranged from 5 to 50CTCs in 1 mL of blood [77]. Recently, Wu et al. fabricated SERSNPs for direct detection of CTCs in the blood with excellent specificity and high sensitivity [78]. The AuNPs were encoded with a Raman reporter molecule, 4-mercaptobenzoic acid (4-MBA), and then functionalized with reductive bovine serum albumin (rBSA) to stabilize the 4-MBA-encoded AuNPs (AuNP-MBA) and decrease the nonspecific interaction with blood cells. Then AuNP-MBA-rBSA-FA composite NPs were constructed with a targeted ligand folic acid (FA) (Fig. 4(A) and (B)). The FA on the surface of AuNP-MBA-rBSA-FA NPs was recognized by CTCs, which over expressed late receptor alpha (FR $\alpha$ ). The protection layer of rBSA was much thinner than that of the reported PEG, resulting in a stronger SERS signal (Fig.4(C)).

For detection of the biological macromolecules such as bacteria pathogen and enzyme, SPR with the advantage of label free provides a powerful platform [79,80]. There are many successful examples of SPR sensing as a medical diagnostic tool, which have been reported for biomarkers, pathogen detection and hormone analysis with high sensitivity. For example, Mc Phillips et al. employed aligned Au nano tube arrays to strengthen performance of refractive index sensors in biomolecular binding reactions [81]. Generally, sandwich [82] and competitive or inhibition assay [83] are two major detection approaches in SPR biosensor. In 2012, Fernandez et al. demonstrated that AuNMs combined with sandwich assays could improve detection sensitivity and selectivity of protein detection [84]. Jung et al. [85] introduced a strategy for enhancement of SPR signals by adopting AuNPs and a SiO<sub>2</sub> layer on a Au surface. The modified surfaces showed significant changes in SPR signal when biomolecules were attached to the surface as compared with an unmodified Au surface. The LOD of AuNPs immobilized on a SPR chip was 0.1 ng mL<sup>-1</sup> for the prostate specific antigen (PSA), a cancer marker. The enhanced shift of the absorption curve resulted from coupling of the surface and particle Plasmon by the SiO<sub>2</sub> layer and the AuNPs on the gold surface. Now, there were a lot of reports of SPR sensors based on spherical AuNMs for detection of biomolecules [86,87]. The anti-*E.coli* O157:H7 polyclonal antibodies (pAb) were labeled with AuNPs, which were used as secondary antibodies. The *E.coli* O157:H7 was detected using direct assay and enhancing sandwich assay based on the two channels SPR biosensor. By introducing AuNPs-PAB compound, the LOD was determined to be 10 cfu/mL. The sensitivity was 100 times higher than that of direct detection [88]. Compared with spherical AuNMs, AuNRs labels are more favorable for the

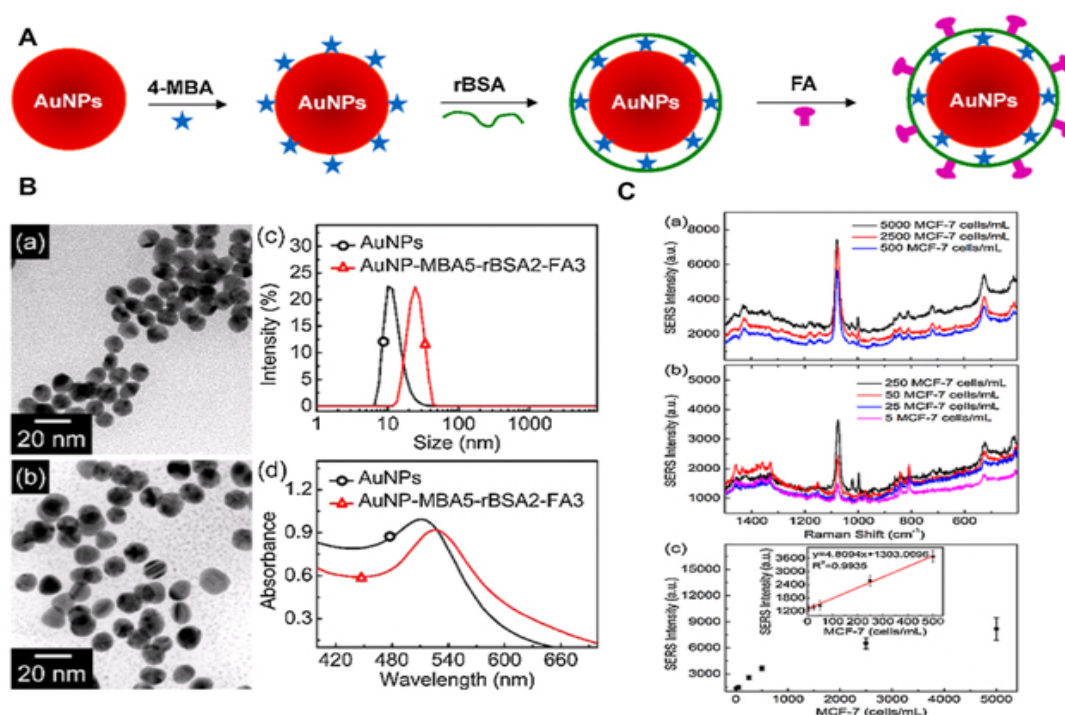


**Fig. 4.** (A) Schematic Illustration for the Design of SERS Nanoparticles. (B) Characterization of the AuNPs (control) and SERS nanoparticles. TEM images of AuNPs (a) and AuNP-MBA5-rBSA2-FA3 (b). (c) Size distributions of AuNPs and AuNP-MBA5-rBSA2-FA3 in Milli-Q water at room temperature. (d) UV-vis spectra of AuNPs and AuNP-MBA5-rBSA2-FA3. (C) Detection sensitivity of the AuNP-MBA5-rBSA2-FA3 nanoparticles for MCF-7 cells in the rabbit blood. Printed with permission from [78]. Copyright 2015 American Chemical Society.

Au-amplified SPR biosensors because of the tunable longitudinal plasmonic peak enables an effective plasmonic coupling between sensing film and NPs. Law et al. revealed the potential of applying this “perfectly matched” nanotag in a well-established SPR sensing system and immunoassay. Through detection of tumor necrosis factor alpha antigen, 40-fold sensitivity enhancement using wavelength-matched AuNRs was observed [89]. Recently, Xianget al [90]. developed a SPR DNA biosensor array based on target-primed rolling circle amplification (RCA) for isothermal and rapid detection of two pathogenic mycobacterium, mycobacterium tuberculosis complex (MTBC) and mycobacterium avium complex (MAC) (Fig. 5). AuNPs were directly assembled on to the surface of the sensor chip via hexanedithiol (HDT) for enhancement of sensitivity as a label-free detection system. Experimental results showed that the signal enhancement by the target-primed RCA together with AuNPs-embedded surface caused at least 10-fold increased sensitivity as compared with conventional RCA on bare SPR chip method.

Besides, the chemical vapor deposition (CVD) method has been adopted by Ruoff’s group for large-scale preparation of high-quality graphene sheets [91]. The strategy based on AuNMs combined with graphene sheets could improve the conductivity of SPR [92]. In 2013, Zhang et al. employed Au-graphene oxide composite in the wavelength modulation SPR biosensor for rabbit

IgG detection [93]. In their study, the staphylococcal protein A (SPA) modified Au-graphene oxide composite was directly immobilized onto SPR chips without any additional chemical treatment. The biosensor with the SPA modified Au-graphene oxide composite as the enhanced sensing platform exhibited a satisfactory response to rabbit IgG. The LOD obtained with the composite was 16 times lower than that obtained with the SPA modified chip. This study provided a simple and effective approach for fabrication of sensitive SPR immunosensors and extended the application of the Au-graphene oxide composite in immunoassays.

Molecularly imprinted polymers (MIPs) have become a competitive tool in the field of molecular recognition, owing to their low-cost, physical robustness, thermal stability and easy preparation over biological receptors and other functionalized materials [3]. High surface-to-volume ratio makes AuNPs a competitive candidate as matrix material for novel nanosized MIPs. Xie et al. showed a surface molecular self-assembly strategy for MIP in electro polymerized aminothiophenol (ATP) membranes at the AuNP-modified glass carbon electrode for electrochemical detection of pesticidechlorpyrifos [94]. Yu et al. constructed an EC sensor for determination of dopamine based on core-shell composite of AuNPs and SiO<sub>2</sub> MIPs through sol-gel technique [95]. Similarly, Xue et al. prepared a highly sensitive and selective biomimetic EC sensor for amperometric detection of trace dopamine (DA)

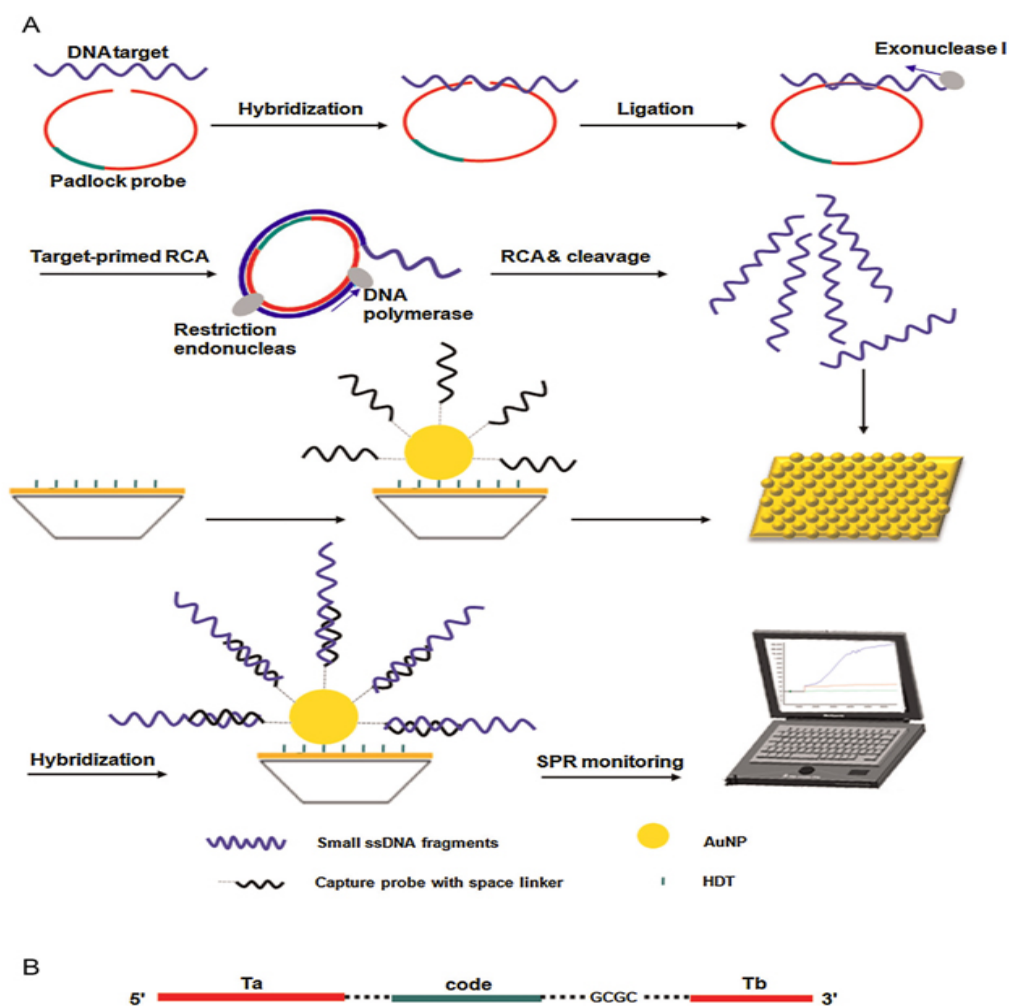


**Fig. 5.** (A) Principle of target-primed RCA-cleavage reaction-based AuNP-embedded SPR assay. (B) Mode of the padlock probe. Ta and Tb are asymmetric target complementary regions in padlock probe. Each padlock probe contains a unique code sequence for multiplex hybridization. The dotted line represents the bases in the linker sequence. Printed with permission from [90]. Copyright 2015 Elsevier.

in human serums by AuNPs doped MIPs (Fig 6). The LOD of the proposed EC sensor for DA was 7.8 nmol/L [96]. Sun et al. [97] presented an EC sensor for detection of 3-chloro-1, 2-propanediol (3-MCPD) that was usually used as surfactant. They fabricated an AuNPs-modified glassy carbon electrode coated with an MIP film via electro polymerization. The LOD reached  $3.8 \times 10^{-18}$  mol/L. impressively, the sensor showed high sensitivity, good selectivity, excellent reproducibility and stability during the quantitative determination of 3-MCPD.

Ultrasensitive detection of biomolecules (especially for disease markers) is very important for early disease diagnosis. To realize ultrasensitive detection of biomolecules, development of novel and robust detection methods for signal amplification of EC sensors is essential. In past work, a lot of photo- or electro-active indicators, such as ferrocene [98], methylene blue [99] and enzymes [100], were immobilized onto AuNPs to realize the detection signals amplification. Zheng et al. prepared an ultrasensitive EC sensor

based on network-like thiocyanuric acid/AuNPs for detection of thrombin [101]. Zhao et al. fabricated an ultrasensitive and highly specific EC aptasensor for thrombin based on amplification of aptamer-AuNPs-horseradish peroxidase conjugates [102]. He et al. reported a label-free and sensitive signal-on electrochemical assay for MTase quantification and activity analysis using AuNP amplification [103]. In 2016, an ultrasensitive DNA biosensor was developed through in situ labeling of electro active melamine-Cu<sup>2+</sup> complex (Mel-Cu<sup>2+</sup>) on the end of hairpin-like probe using AuNPs as the signal amplification platform by our group [104]. In this work, the highly conductive AuNPs were applied as the loading platform of the Mel-Cu<sup>2+</sup> tags. The proposed biosensor showed high selectivity, wide linear range and low LOD for target DNA.

Except for the aforementioned amplification strategies, rolling circle amplification (RCA) is one of the most popular and important amplification strategies. Therefore, the dual amplification strategies combined RCA with DNA-AuNPs probe could tremendously

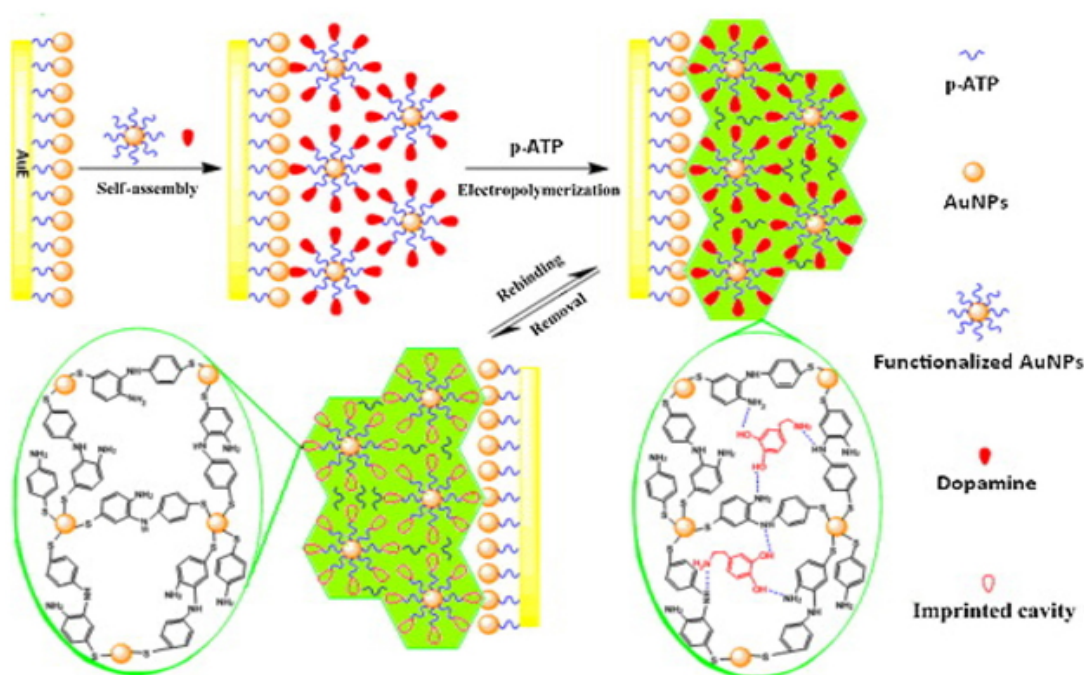


Fig. 6. Scheme of preparation of AuNPs@MIES. Printed with permission from [96]. Copyright 2013 Elsevier.

improve the sensitivity of bacterial detection. Zhu et al. reported an electrochemical sensing strategy for ultrasensitive and rapid detection of Salmonella by combining the RCA with DNA-AuNPs probe [105]. As shown in Fig 7, the target DNA could be specifically captured by probe 1 on the sensing interface. Then the circularization mixture was added to form a typical sandwich structure. In the presence of dNTPs and phi29 DNA polymerase, the RCA was initiated to produce micrometer-long single-strand DNA. Finally, the detection probe (DNA-AuNPs) recognized RCA product to produce enzymatic electrochemical signal. The developed method was successfully applied to detect Salmonella with lower LOD of 6CFU mL<sup>-1</sup> in real milk sample.

Both of graphene based materials and AuNPs are the frequently used nonmaterial in the field of EC biosensors for detection of biomolecules due to their excellent electrical signal amplification and the versatile fictionalization chemistry. Accordingly, hybrid nonmaterial sensors based on AuNPs distributing on the surface of graphene oxide (GO) or reduce GO (rGO) also attract much scientific interest [106,107]. The most frequently used technique refers to reaction of AuCl<sub>3</sub> with GO under reductive condition for *in situ* anchoring AuNPs to GO or rGO. This method, however, often lacks fine control over the size, uniformity and density of AuNPs on the GO sheets in the reaction process [108]. AuNPs can be decorated to GO surface based on NH-Au binding [109] or SH-Au binding [110]. DNA [111] and proteins [112] have been also used as the molecular linkers between AuNPs and GO. These methods have greatly increased the uniformity and density of AuNPs. Liu et al. presented stable label-free EC sensor for detection of cardiac

troponin-I (cTnI) in the early diagnosis of myocardial infarction based on AuNPs and GO nanocomposites [113]. The EC sensor demonstrated good selectivity and high sensitivity against human-cTnI, and was capable of detecting cTnI at concentrations as low as 0.05 ng mL<sup>-1</sup>, which was 100 times lower than that by conventional methods. Karaboga et al. described a simple and disposable immunosensor based on indium-tin-oxide (ITO) sheets modified with AuNPs to sensitively analyze heat shock protein70 (HSP70), a potential biomarker that could be evaluated in diagnosis of some carcinomas [114]. Wang et al. constructed an AuNPs/polyaniline/chitosan-graphene sheets based electrochemical DNA sensor with functional hairpin probe for detection of BCR/ABL fusion gene in chronic myelogenous leukemia [115]. Recently, the interest in layered transition metal chalcogenides, especially MoS<sub>2</sub>, has been growing quickly because they share many impressive physicochemical properties of graphene. Su et al. have prepared an EC sensor based on MoS<sub>2</sub> layer for sensitive detection of proteins [116]. In subsequent work, they further fabricated a MoS<sub>2</sub>-based EC aptasensor for simultaneous detection of thrombin and adenosine triphosphate (ATP) based on AuNPs-MoS<sub>2</sub> nano composites [117].

Development of novel ultrasensitive EC sensors provides a great opportunity for quick and specific sensing of cancer molecular markers (CMMs), which early detection is of great importance for the success of cancer therapy [118]. Johari-Ahar et al. [119] modified an Au electrode with mercapto propionic acid (MPA), and then consecutively conjugated with silica coated AuNPs (AuNPs@SiO<sub>2</sub>), CdSe QDs and anti-CA-125 monoclonal antibody (mAb). Successive conjugation of AuNP@SiO<sub>2</sub>, CdSe QD and anti-



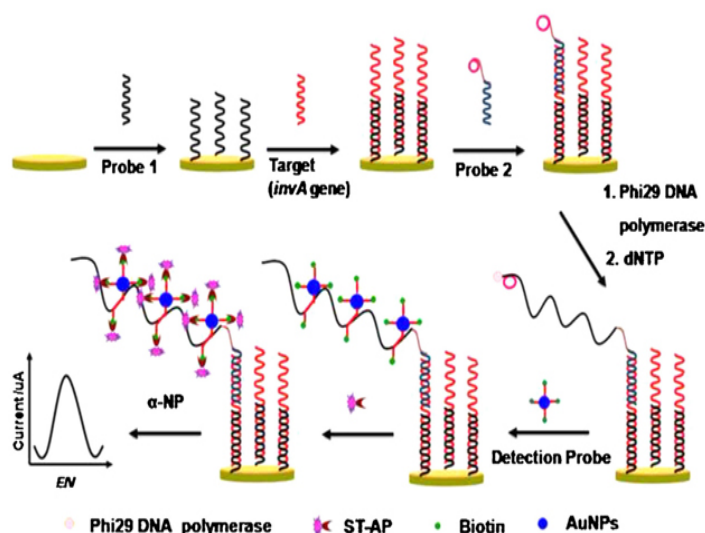


Fig. 7. Scheme of the designed strategy for detection of Salmonella. Printed with permission from [105]. Copyright 2014 Elsevier.

CA-125 mAb onto the Au electrode resulted in sensitive detection of CA-125 with a LOD of 0.0016 U mL<sup>-1</sup>. Serafin et al. presented an immuno reagent label-free strategy to construct a dual EC immunosensor using carbon nanotube screen printed electrodes modified with AuNPs and PEDOT NPs for the multiplexed determination of human growth hormone and prolactin [120].

The ECL of luminol promoted by AuNMs was reported by Cui et al [121]. The ECL intensity of luminol was found to be enhanced by ~2 to 3 orders with catalysis of AuNPs. Li et al. proposed a simple and sensitive sandwich-type ECL immunosensor for detection of cancer antigen 125 on a nonporous Au modified glassy carbon electrode [122]. Gao et al. prepared an ultrasensitive luminol ECL immunosensor by using carboxyl group functionalized MWCNTs as platform and glucose oxidase supported on AuNPs decorated MWCNTs as labels [123]. The results indicated that this developed sensor exhibited sensitive and stable response for detection of α-1-fetoprotein (AFP), ranging from 0.0001 to 80 ng mL<sup>-1</sup> with a LOD down to 0.03 pg mL<sup>-1</sup>. Gui et al. constructed a simple and sensitive ECL biosensor for determination of β-lactamase with Ru(phen)<sub>2</sub>(cpaphen)<sup>2+</sup> linked-ampicillin (Ru-Amp) [124]. In their work, Ru-Amp complex act not only as a specific recognition element for β-lactamase but also as the ECL luminescent reagent. The biosensor displayed excellent sensitivity of a concentration variation from 50 pg mL<sup>-1</sup> to 100 ng mL<sup>-1</sup> with a high sensitivity of 37 pg mL<sup>-1</sup>. Besides the organic dye, noble metal NPs could greatly affect ECL behavior of semiconductor QDs [125]. The ECL enhancement by LSPR of AuNPs was investigated and termed as surface enhanced ECL (SEECCL) [126]. The LSPR of AuNPs was found to increase both the excitation rate and the emission factor of luminophores, and thus the ECL intensity was enhanced greatly. Based on this SEECCL effect, a method was developed for

ultrasensitive detection of Hg<sup>2+</sup> in drinking water [127]. Moreover, a SEECCL sensor was prepared for detection of carcinoembryonic antigen(CEA). In this sensor, Ru(bpy)<sub>3</sub><sup>2+</sup>-doped SiO<sub>2</sub>NPs (Ru@SiO<sub>2</sub>) act as ECL luminophores, while AuNPs were used as LSPR source to enhance the ECL signal. Two different types of aptamers specific to CEA were modified on the surface of Ru@SiO<sub>2</sub> and AuNPs, respectively. A LOD of 1.52 × 10<sup>-6</sup>ng/mL of CEA in human serum was achieved [128].

Electrochemical kinase analysis is of special interest in monitoring biological activity in process of life. Measurements of phosphorylation reactions based on oxidation current of electro active species such as tyrosine [129], ferrocene [130], etc., which are conjugated on the substrate during the phosphorylation processes, have been reported [131]. To simplify the detection procedure, AuNPs labeled phosphorylation process for the kinase assay was designed by measuring the redox currents of AuNPs [132]. However, the sensitivity of the developed method was relatively low. In order to improve the analytical performance, a DNA-based strategy was also described by the chronocoulometric response of [Ru(NH<sub>3</sub>)<sub>6</sub>]<sup>3+</sup> absorbed on the DNA-AuNPs that linked with the phosphorylated peptide by Zr<sup>4+</sup> [133]. Despite the improvement of these methods, it still remains great challenge to develop sensitive, accurate and rapid methods for the profiling of kinase activity and inhibition. Most recently, Wang et al. built a highly sensitive EC sensor for monitoring kinase activity based on DNA induced AuNPs polymeric network block signal amplification [134]. In this strategy, the current signal of EC sensor was significantly amplified to afford a highly sensitive electrochemical analysis of kinase activity, due to its excellent electro activity and high accommodation of the DNA AuNPs polymeric network block for [Ru(NH<sub>3</sub>)<sub>6</sub>]<sup>3+</sup>. Notably, the proposed EC sensor presented a low LOD of 0.03 U mL<sup>-1</sup> for protein kinase A (PKA) activity and excellent stability even in celllysates and serum samples. Jing et al. developed a sensitive and selective electrochemical method for detection of DNA methylation as well as determination of DNA methyl transferase (MTase) activity and screening of MTase inhibitor [135]. In this work, methyleneblue (MB) was employed as electrochemical indicator and DNA-modified AuNPs were used as signal amplification unit because the DNA strands in this composite had strong adsorption ability toward MB (Fig. 8). The differential pulse voltammetry signal demonstrated a linear relationship with logarithm of DNA methylation concentration ranging from 0.075 to 30 U/mL, achieving a LOD of 0.02 U/mL.

Overall, the LSPR feature and excellent biocompatibility of AuNMs provide great chance for improving the analytical performance of EC sensors. Currently, only spherical AuNPs have been extensively applied into fabrication of EC sensor. Certainly, other shaped AuNMs possesses specific physiochemical property, and may offer addition-

al application option in signal amplification of ECL or EC sensors.

### AuNMs Based Imaging

Recently, AuNMs have been highlighted in biological imaging as a contrast agent due to their unique optical property [136]. Biological imaging with simultaneous diagnosis and therapy will provide the multimodality needed for accurate targeted therapy [137]. AuNMs have been considered as one of the best contrast agents for disease diagnosis, and functionalization of AuNMs becomes essential for application of AuNMs in computed tomography (CT), X-ray and SERS imaging [138].

As one of the most reliable imaging modes, CT has been widely used owing to its high spatial and density resolution. For CT imaging, contrast agents are generally required to increase the density of the area to be imaged to improve the diagnostic accuracy. The commercially available CT imaging agents used in clinics are usually iodinated small molecules (e.g. omnipaque) that have severe drawbacks such as renal toxicity at a high concentration, short imaging time and non-specificity [139]. For improved CT imaging, some inorganic NPs such as AuNPs [140,141] have been used as contrast agents because of their higher X-ray attenuation coefficients than those of iodine-based small molecular agents.

AuNPs radio sensitization represents a novel technique in enhancement of ionising radiation dose and its effect on biological systems [142]. From the first demonstration of AuNPs as a radiation contrast agent, AuNPs radio enhancement/sensitization has become an increasing area of investigation as an approach to increase the effectiveness of ionizing radiation in biological systems [143]. For example, dendrimers of well-defined structure have been used as templates or stabilizers to form dendrimer-entrapped AuNPs [144,145] for CT imaging applications, especially for blood pool imaging and tumor imaging. Peng et al. reported a facile approach to synthesize the dendrimer-stabilized AuNPs through use of amine-terminated fifth-generation poly(amidoamine) (PAMAM) dendrimers modified by diatrizoic acid as stabilizers for enhanced CT imaging [146]. Li et al. constructed Au-coated iron oxide ( $Fe_3O_4@Au$ ) nanoroses to integrate five distinct functions including aptamer-based targeting, magnetic resonance imaging (MRI), optical imaging, photo thermal therapy and chemotherapy into one single probe [147]. Zhang et al. introduced design and synthesis of branched polyethylene mine (PEI)-stabilized AuNPs modified with polyethylene glycol (PEG) for blood pool, lymph node and tumor CT imaging [148].

Despite recent advances on the different shapes of AuNPs in

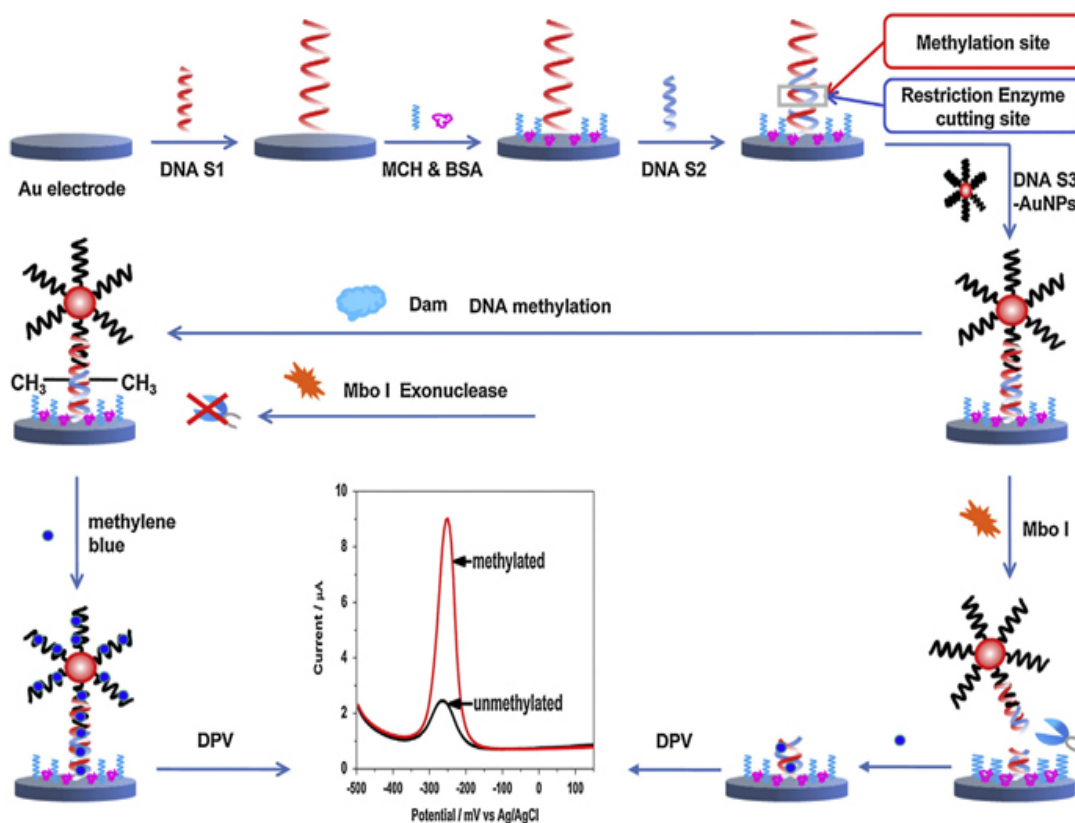
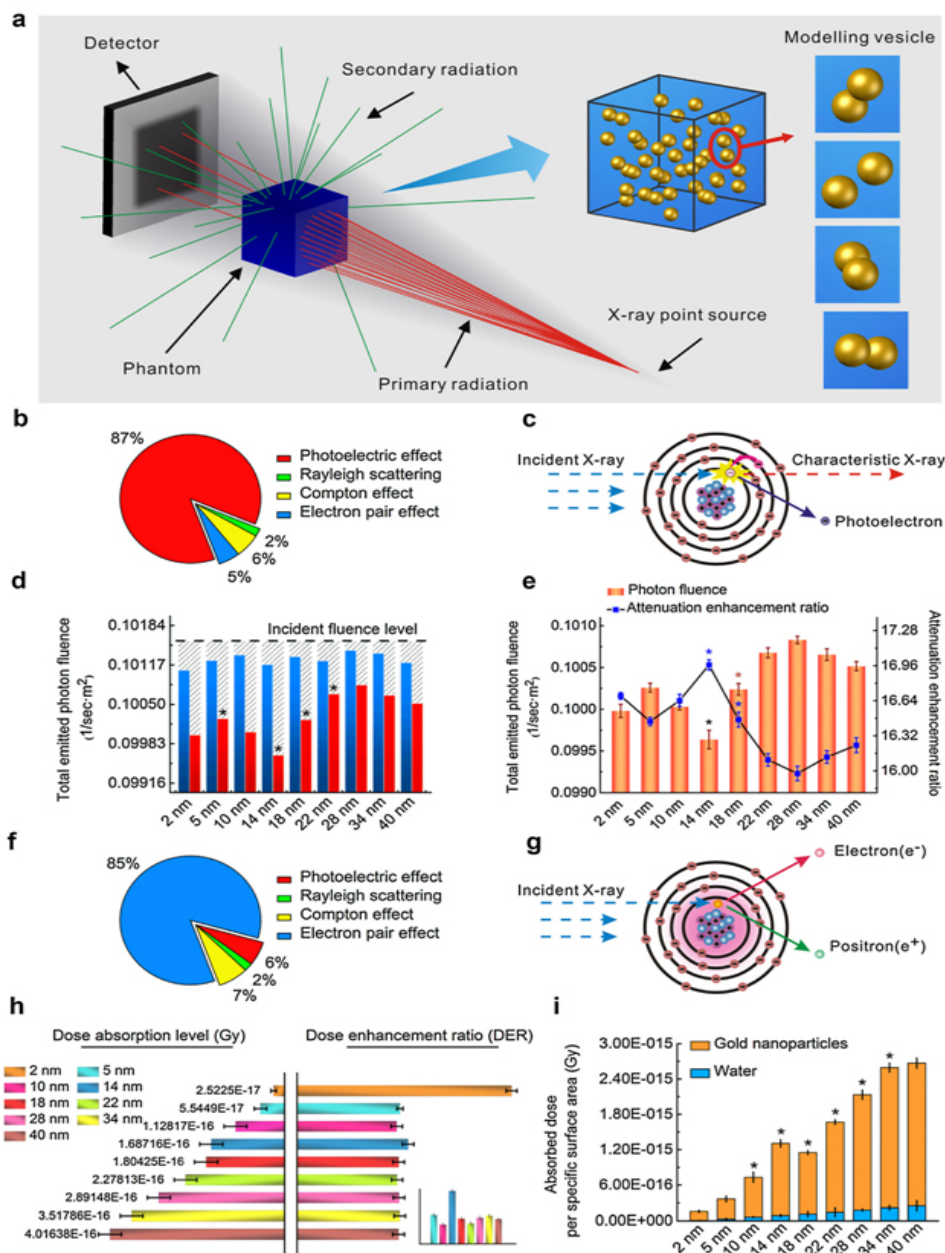


Fig. 8. Scheme of the developed method for detection of DNA methylation and assay of DNA methyltransferase activity. Printed with permission from [135]. Copyright2014 Elsevier.

improving CT attenuation differences or radiotherapy damage of tumors, few studies have systematically investigated the size effect of spherical AuNPs on CT imaging and radio sensitization [149,150]. In most cases, AuNPs concentration effect was examined for evaluating enhancement performances [151]. Some published results indicated that great difference existed even with the same con-centration of AuNPs with different size [152]. In 2016, Dou et

al. explored and confirmed the distinctive size-dependent effects based on a series of spherical AuNPs for enhanced CT imaging and radiotherapy (Figure 9) [153].

The result indicated that AuNPs had great size-dependent enhancement on CT imaging and radiotherapy (RT) in the size range of 3–50 nm. Interestingly, AuNPs with a size of ~13 nm could



**Fig. 9.** Monte Carlo simulation to evaluate size-dependent enhancement. (a) Scheme showing a phantom filled with a AuNP aqueous suspension that may trigger completely different secondary radiation depending on primary radiation energy irradiated from the X-ray point source for CT detection or radiotherapy. A simulated “modeling vesicle” containing two particles randomly distributed, representative of the system inhomogeneity based on particle sizes. (b) X-ray attenuation mainly coming from a photoelectric effect under the kilovoltage energy radiation for CT imaging, with little influence by other interactions including Rayleigh scattering, Compton scattering and electron pair effect. (c) Photoelectric effect generation. Inner-shell electrons receive energy from the incident X-rays, which are subsequently ejected from the atom as a photoelectron,

simultaneously possess superior CT contrastability and significant radioactive disruption.

AuNPs have been studied as potential contrast agents for X-ray imaging, because they are nontoxic and have a higher atomic number and X-ray absorption coefficient compared with typical iodine-based contrast agents [154]. Rand et al. proposed that the enhanced sensitivity of the X-ray scatter imaging technique over that of typical absorption based X-ray imaging could reduce the amount of AuNPs required for visible contrast [155]. Therefore, they developed an imaging technique for the early diagnosis of hepato cellular carcinoma that utilized surface-modified AuNPs in combination with X-ray imaging. Tissues labeled with these electron-dense particles showed enhanced X-ray scattering over normal tissues, distinguishing cells containing AuNPs from cells without Au in X-ray scatter images. This approach could enable in vivo detection of tumors as small as a few millimeters in size. In 2012, Chien et al. used AuNPs as high-resolution X-ray imaging contrast agents for analysis of tumor-related micro-vasculature [156].

AuNMs hold great interest in imaging field thanks to their characteristics such as monodispersity, stability, minimal toxicity and excellent contrasting for transmission electron microscopy (TEM) analysis, which enable tracking with unprecedented resolution on dynamic of uptake, intracellular sorting and potential secretion [157,158]. Recent results gathered on the interaction of AuNPs with different synthetic lipid membranes [159] or cell lines demonstrate that not only properties such as size, charge and chemical functionality, but also the arrangement of organic ligands on NP surface, dictate the internalization route [160]. Moreover, surface functionalization may influence the fate of AuNP upon cell uptake, for instance, HUVEC cells treated with AuNPs coated by different peptides display distinct exocytosis profiles [161]. Recently, Marchesano et al. observed inward and outward trafficking of AuNPs at whole animal level using the small invertebrate *Hydra vulgaris* [162].

AuNPs are also excellent candidates as contrast agents for SERS imaging. Yigit et al. synthesized conjugates of AuNMs and 3,3-diethylthiatricarbocyanine iodide (AuNM-DTTC) that were used as a bimodal contrast agent for in vivo MRI and Raman spectroscopy [163]. The probe consisted of MRI-active super paramagnetic iron oxide NPs, stably complexed with AuNM-DTTC. The Au component served as a substrate for a Raman active dye molecule to generate a SERS effect. The synthesized probe produced T2 weighted contrast and was simultaneously used as a SERS active material both in silico and *in vivo*. Kong et al. prepared metal carbonyl based bio tags by combining osmium carbonyl clusters and AuNPs, as an example of an organo metallic-AuNPs (OM-AuNPs) conjugate used to cell SERS imaging [164]. It showed clearly the advantage of transition-metal carbonyl compounds, for

which the CO stretching vibration signal was well separated from other molecular vibrational modes of the cells in live-cell imaging.

### Disadvantage of Using AuNMs

A big disadvantage of using AuNMs as the optical contrast agents is their high photo thermal conversion efficiency under resonance excitation, which may perturb or even damage the biological species being imaged [165]. Thus, to minimize unwanted heating in bioimaging applications, laser irradiation time is typically set to be in the range of 0.1–10 S, which either lowers the SERS signal contrast or is simply not suited for image-guided tumor resection in intraoperative settings, considering the longer timescales (1–2 h) associated with such procedures [166,167]. While resonant nanostructures are certainly desirable for the diagnostic applications, having the ability to tune the photo thermal effect of SERS probes while preserving their high SERS activity is critical to avoid unwanted heating during imaging. Oh et al. designed and synthesized plasmonic AuNPs with ultra small (typically, ~1 nm) interior gap using thiolated DNA and obtained the relationships between these noble metal nanogap structures and plasmonic signals from these structures [168]. In 2015, Tian et al. demonstrated bioenabled synthesis of a novel class of ultra-bright SERS probes with built-in and accessible electromagnetic hotspots formed by densely packed satellite NPs grown on a plasmonic core [169]. Through the rational choice of the shape of the core, the LSPR wavelength of Au superstructures was tuned to be either off- or on-resonant with the NIR excitation without sacrificing their high SERS activity. Consequently, the photo thermal efficiency of these ultra-bright SERS tags could be tuned to realize either contrast agents with minimal heating and perturbation, or multifunctional diagnostic agents that imaged and photo thermally killed the targeted cells.

### Conclusions

1. The outstanding characteristics of AuNMs make them promising candidates as the signal reporters, enhancement materials or others involved with bioassay, food safety, environmental monitoring and medical science.
2. A series of novel and sophisticated synthesis methods for AuNMs have been developed, but how to precisely control them on dispersed size and morphology and to achieve high quality of AuNMs with vivid color (LSPR) is still a crucial but challenging issue for their application in analytical science. The AuNMs with precisely-controlled vivid color possess abundant optical information and can encode biological or chemical recognition units to develop robust analytical methods in food safety, clinic diagnosis and so on. In addition, we are far from controllable assembly of AuNMs into the desirable structures of the collective properties [170].

3. AuNMs have shown excellent performance in enhancement of SERS signal to improve detection sensitivity. Therefore, AuNMs in combination with other functional metal or organic nonmaterials, such as Si, Al, MOFs and so on, to develop multimodal composite nonmaterial become a new trend in high sensitive SERS detection of various target analytes [171,172], as well as in high resolution bioimaging in the future.
- 4- AuNMs offer a rapid, efficient, cost-effective and robust sensing platform for detection of different chemicals and bio-markers due to their unique chemical, physical and optical properties. It is noted that the sensitive, stable and multiplex assay of target analytes is highly desirable. To meet these requirements, new multifunctional AuNMs must be developed and used as LFICA label, colorimetric sensing readout and signal amplification of EC sensor, etc.
5. AuNCs as excellent fluorescent probe materials have shown great potential in analytical science [173]. However, extensive efforts must be made for developing novel synthesis methods to achieve high quality AuNCs with remarkable QY and extraordinary stability. In addition, the coordination nature of the AuNCs-protection group complexes implies that the stability of metal NCs is affected by the presence of other strong competing ligands in aqueous solution. The intracellular stability of AuNCs hence becomes a serious issue. With development of technologies of synthesis and surface modification, AuNCs will be widely employed as alternatives to conventional fluorophores in analytical science including biosensors, bioimaging and soon.
6. We notice that though many new analytical methods based on AuNMs have been developed in the laboratories, such materials are not used as much in an industrial setting. There must be more scope for these platforms to improve, for example, cost of preparing the AuNMs based sensors, reproducibility of different batches for sensor production, and stability of long-term storage of the AuNMs based sensors, and so on.
7. The mechanism of DNA-guided AuNMs synthesis not only provide deep understanding of the interactions between the DNA and nanomaterials but also allow better control of the shapes and surface properties of many nanomaterials.
8. AuNMs with excellent features have prompted great development of analytical sciences and have stood at a critical juncture, with a vast amount of researches that form a solid foundation for future work. Great deals of efforts need to be paid to push on to take AuNMs-based analytical technologies from lab to market.

## References

1. Madkour LH (2017) Vision for life sciences: interfaces between nano-electronic and biological systems. *Glob Drugs Therap* 2(4): 1-4. doi: 10.15761/GDT.1000126

2. Sardar R, Funston AM, Mulvaney P, Murray RW (2009) Gold nanoparticles: past, present, and future. *Langmuir* 25(24): 13840-13851.
3. Wang P, Sun X, Su X, Wang T (2016) Advancements of molecularly printed polymers in the food safety field. *Analysts* 141: 3540-3553.
4. Zhang, L Wang E (2014) *Nano Today* 9: 132-157.
5. Ballou S, Goodpaster J, MacCrehan W, Reeder D (2003) Forensic analysis. *Anal. Bioanal Chem* 376(8): 1149-1150.
6. Burnworth M, Rowan SJ, Weder C (2007) Fluorescent sensors for the detection of chemical warfare agents. *Chem Eur J* 13(28): 7828-7836.
7. Zhang Z, Liu J, Feng T, Yao Y, Gao L, et al. (2013) Time-Resolved Fluoroimmunoassay as an Advantageous Analytical Method for Assessing the Total Concentration and Environmental Risk of Fluoroquinolones in Surface Waters Environ. *Sci Technol* 47(1): 454-462.
8. Anker JN, Hall WP, Lyandres O, Shah NC, Zhao J, et al. (2008) Biosensing with plasmonic nanosensors. *Nat Mater* 7: 442-453.
9. Debouttière PJ, Roux S, Vocanson F, Billotey C, Beuf O, et al. (2006) Design of Gold Nanoparticles for Magnetic Resonance Imaging Tillement *AdvFunct Mater* 16(18): 2330-2339.
10. Qian X, Li J, Nie S (2009) Stimuli-Responsive SERS Nanoparticles: Conformational Control of Plasmonic Coupling and Surface Raman Enhancement. *J Am Chem Soc* 131(22): 7540-7541.
11. Thomas KG, Kamat PV (2000) Making Gold Nanoparticles Glow: Enhanced Emission from a Surface-Bound Fluorophore. *J Am Chem Soc* 122(11): 2655-2656.
12. Ipe BI, Yoo S K, Thomas KG (2006) Functionalized Gold Nanoparticles as Phosphorescent Nanomaterials and Sensors. *J Am Chem Soc* 128(6): 1907-1913.
13. Kisailus D, Najarian M, Weaver JC, Morse DE (2005) Functionalized Gold Nanoparticles Mimic Catalytic Activity of a Polysiloxane-Synthesizing Enzyme *Adv Mater* 17(10): 1234-1239.
14. Qian X, Peng XH, Ansari DO, Yin Goen Q, Chen GZ, et al. (2008) In vivo tumor targeting and spectroscopic detection with surface-enhanced Raman nanoparticle tags. *Nat Biotechnol* 26(1): 83-90.
15. Haghghi B, Bozorgzadeh S (2011) Enhanced Electrochemiluminescence From Luminol at Multi-Walled Carbon Nanotubes Decorated With Palladium Nanoparticles: A Novel Route for the Fabrication of an Oxygen Sensor and a Glucose Biosensor. *Anal Chim Acta* 697(1-2): 90-97.
16. Tang J, Tang DP, Su BL, Huang JX, Qiu B, et al. (2011) Enzyme-free electrochemical immunoassay with catalytic reduction of *p*-nitrophenol and recycling of *p*-aminophenol using gold nanoparticles-coated carbon nanotubes as nanocatalysts. *BiosensBioelectron* 26(7): 3219-3226.
17. Zhu YP, Chandra P, Song KM, Ban C, Shim YB (2012) Label-free detection of kanamycin based on the aptamer-functionalized conducting polymer/gold nanocomposite. *BiosensBioelectron* 36(1): 29-34.
18. Sun X, Li F, Shen G, Huang J, Wang X (2014) Aptasensor based on the synergistic contributions of chitosan-gold nanoparticles, graphene-gold nanoparticles and multi-walled carbon nanotubes-cobalt phthalocyanine nanocomposites for kanamycin detection. *Analyst* 139: 299-308.

19. Roushani M, Shahdostfard F (2015) A Highly Selective and Sensitive Cocaine Aptasensor Based on Covalent Attachment of the Aptamer-Functionalized AuNPs Onto Nanocomposite as the Support Platform. *Anal ChimActa* 853: 214-221.
20. Wang Y, Knoll W, Dostalek J (2012) Bacterial Pathogen Surface Plasmon Resonance Biosensor Advanced by Long Range Surface Plasmons and Magnetic Nanoparticle Assays *Anal Chem* 84(19): 8345-8350.
21. Yang X, Wang Q, Wang K, Tan W, Li H (2007) Enhanced surface plasmon resonance with the modified catalytic growth of Au nanoparticles. *BiosensBioelectron* 22: 1106-1110.
22. Jung J, Na K, Lee J, Kim KW, Hyun J (2009) Enhanced surface plasmon resonance by Au nanoparticles immobilized on a dielectric  $\text{SiO}_2$  layer on a golden surface. *Anal ChimActa* 651(1): 91-97.
23. Shen L, Chen Z, Li YH, He SL, Xie SB, et al. (2008) Electrochemical DNAzyme Sensor for Lead Based on Amplification of DNA-Au Bio-Bar Codes. *Anal Chem* 80(16): 6323-6328.
24. Tang SR, Tong P, Lu W, Chen JF, Yan ZM, et al. (2014) A novel label-free electrochemical sensor for  $\text{Hg}^{2+}$  based on the catalytic formation of metal nanoparticle. *BiosensBioelectron* 59: 1-5.
25. Wang N, Lin M, Dai H, Ma H (2016) Functionalized Gold Nanoparticles/Reduced Graphene Oxide Nanocomposites for Ultrasensitive Electrochemical Sensing of Mercury Ions Based on Thymine-Mercury-Thymine Structure. *BiosensBioelectron* 79: 320-326.
26. Wang S, Wang Y, Zhou L, Li J, Wang S, et al. (2014) Fabrication of an effective electrochemical platform based on graphene and AuNPs for high sensitive detection of trace  $\text{Cu}^{2+}$ . *Electrochim Acta* 132: 7-14.
27. Yang Y, Zhang S, Kang M, He L, Zhao J, et al. (2015) Anal Biochem Selective Detection of Silver Ions Using Mushroom-Like Polyaniline and Gold Nanoparticle Nanocomposite-Based Electrochemical DNA Sensor. *Anal Biochem* 490: 7-13.
28. Kimling J, Maier M, Okenve B, Kotaidis V, Ballot H, et al. (2006) Turkevich Method for Gold Nanoparticle Synthesis Revisited. *J PhysChemB* 110(32): 15700-15707.
29. Kumar S, Gandhi KS, Kumar R (2007) Modeling of Formation of Gold Nanoparticles by Citrate Method *IndEngChem Res* 46(10): 3128-3136.
30. Schmid G (1992) Large clusters and colloids. Metals in the embryonic state. *Chem Rev* 92(8): 1709-1727.
31. Schmid G, Chi LF (1998) Metal Clusters and Colloids. *Adv Mater* 10(7): 515-526.
32. Brust M, Fink J, Bethell D, Schiffrin DJ, Kiely CJ (1995) Synthesis and reactions of functionalised gold nanoparticles. *J ChemSoc Chem Commun* 1655-1656.
33. Saha K, Agasti SS, Kim C, Li X, Rotello VM (2012) Gold nanoparticles in chemical and biological sensing. *Chem Rev* 112(5): 2739-2779.
34. Daniel MC, Astruc D (2004) Gold Nanoparticles: Assembly, Supramolecular Chemistry, Quantum-Size-Related Properties, and Applications toward Biology, Catalysis, and Nanotechnology. *Chem Rev* 104(1): 293-346.
35. Burda C, Chen X, Narayan R, El-Sayed MA (2005) Chemistry and Properties of Nanocrystals of Different Shapes. *Chem Rev* 105(4): 1025-1102.
36. Skrabalak SE, Chen J, Au L, Lu X, Li X, et al. (2007) Gold Nanocages for Biomedical Applications. *Adv Mater* 19(20): 3177-3184.
37. Sun Y, Xia Y (2002) Shape-controlled synthesis of gold and silver nanoparticles. *Science* 298(5601): 2176-2179.
38. Malikova N, Pastoriza-Santos I, Schierhorn M, Kotov N, Liz-Marzan L, et al. (2002) Layer-by-Layer Assembled Mixed Spherical and Planar Gold Nanoparticles: Control of Interparticle Interactions. *Langmuir* 18(19): 3694-3697.
39. Manna L, Milliron D, Meisel A, Scher EC, Alivisatos AP (2003) Controlled growth of tetrapod-branched inorganic nanocrystals. *Nat Mater* 2: 382-385.
40. Cao YW, Jin R, Mirkin CA (2001) DNA-Modified Core-Shell Ag/Au Nanoparticles. *J Am ChemSoc* 123(32): 7961-7962.
41. Zhang L, Niu W, Xu G (2012) Synthesis and application of noble metal nanocrystals with high-energy facets. *Nano Today* 7(6): 586-605.
42. Lai J, Niu W, Luque R, Xu G (2015) *Nano Today* 10: 240-267.
43. Kim F, Song JH, Yang P (2002) Photochemical Synthesis of Gold Nanorods. *J Am ChemSoc* 124(48): 14316-14317.
44. Niu W, Zheng S, Wang D, Liu X, Li H, et al. (2009) Selective Synthesis of Single-Crystalline Rhombic Dodecahedral, Octahedral, and Cubic Gold Nanocrystals. *Am Chem Soc* 131(2): 697-703.
45. Niu W, Chua YAA, Zhang W, Huang H, Lu X (2015) Highly Symmetric Gold Nanostars: Crystallographic Control and Surface-Enhanced Raman Scattering Property. *J Am Chem Soc* 137(33): 10460-10463.
46. Zheng J, Petty JT, Dickson RM (2003) High Quantum Yield Blue Emission from Water-Soluble  $\text{Au}_8$  Nanodots. *J Am ChemSoc* 125(26): 7780-7781.
47. Xie J, Zheng Y, Ying JY (2009) Protein-Directed Synthesis of Highly Fluorescent Gold Nanoclusters. *J Am ChemSoc* 131(3): 888-889.
48. Varnavski O, Ramakrishna G, Kim J, Lee D, Goodson T (2010) Critical Size for the Observation of Quantum Confinement in Optically Excited Gold Clusters. *J Am ChemSoc* 132(1): 16-17.
49. Tang Z, Xu B, Wu B, Germann MW, Wang G (2010) Synthesis and Structural Determination of Multidentate 2,3-Dithiol-Stabilized Au Clusters. *J Am Chem Soc* 132(10): 3367-3374.
50. Yu Y, Luo Z, Chevrier DM, Leong DT, Zhang P, et al. (2014) Identification of a Highly Luminescent  $\text{Au}_{22}(\text{SG})_{18}$  Nanocluster. *J A Chem Soc* 136(4): 1246-1249.
51. Pyo K, Thanthirige VD, Kwak K, Pandurangan P, Ramakrishna G, et al. (2015) Ultrabright Luminescence from Gold Nanoclusters: Rigidifying the Au(I)-Thiolate Shell. *J Am ChemSoc* 137(25): 8244-8250.
52. Tan LH, Xing H, Lu Y (2014) DNA as a Powerful Tool for Morphology Control, Spatial Positioning, and Dynamic Assembly of Nanoparticles. *Acc Chem Res* 47(6): 1881-1890.

53. Wang Z, Tang L, Tan LH, Li J, Lu Y (2012) Discovery of the DNA "Genetic Code" for Abiological Gold Nanoparticle Morphologies. *Angew Chem Int Ed* 51(36): 9078-9082.
54. Song T, Tang L, Tan LH, Wang X, Satyavolu NSR, et al. (2015) DNA-Encoded Tuning of Geometric and Plasmonic Properties of Nanoparticles Growing from Gold Nanorod Seeds. *Angew Chem Int Ed* 54(28): 8114-8118.
55. Tan L, Yue Y, Satyavolu NSR, Ali AS, Wang Z, et al. (2015) Mechanistic Insight into DNA-Guided Control of Nanoparticle Morphologies. *Am Chem Soc* 137(45): 14456-14464.
56. Ye X, Jin L, Cagalayan H, Chen J, Xing G, et al. (2012) Improved Size-Tunable Synthesis of Monodisperse Gold Nanorods through the Use of Aromatic Additives. *ACS Nano* 6(3): 2804-2817.
57. Krishna KS, Navin CV, Biswas S, Singh V, Ham K, et al. (2013) Millifluidics for Time-resolved Mapping of the Growth of Gold Nanostructures. *J Am Chem Soc* 135(4): 5450-5456.
58. Johnston CW, Wyatt MA, Li X, Ibrahim A, Shuster J, et al. (2013) Gold biomineralization by a metallophore from a gold-associated microbe. *Nat Chem Biol* 9: 241-243.
59. Zhang MX, Cui R, Tian ZQ, Zhang ZL, Pang DW (2010) Kinetics-Controlled Formation of Gold Clusters Using a Quasi-Biological System. *Adv Funct Mater* 20(21): 3673-3677.
60. Shin Y, Lee C, Yang MS, Jeong S, Kim D, et al. (2014) Two-dimensional Hyper-branched Gold Nanoparticles Synthesized on a Two-dimensional Oil/Water Interface. *Sci Rep* 4: 6119.
61. Abdelaziz R, Disci-Zayed D, Hedayati MK, Pohls JH, Zillohu AU, et al. (2013) Green chemistry and nanofabrication in a levitated Leidenfrost drop. *Nat Com* 4: 2400.
62. Kim JH, Twaddle KM, Hu J, Byun H (2014) Sunlight-Induced Synthesis of Various Gold Nanoparticles and Their Heterogeneous Catalytic Properties on a Paper-Based Substrate. *ACS Appl Mater Interfaces* 6(14): 11514-11522.
63. Gao C, Zhang Q, Lu Z, Yin Y (2011) Templated Synthesis of Metal Nanorods in Silica Nanotubes. *J Am Chem Soc* 133(49): 19706-19709.
64. Liu J, Qiao S, Hartono SB, Lu G (2010) Monodisperse Yolk-Shell Nanoparticles with a Hierarchical Porous Structure for Delivery Vehicles and Nanoreactors. *Angew Chem Int Ed* 49(29): 4981-4985.
65. Christesen SD (1988) Raman Cross Sections of Chemical Agents and Simulants. *Appl Spectrosc* 42(2): 318-321.
66. Yan J, Su S, He S, He Y, Zhao B, et al. (2012) Nano Rolling-Circle Amplification for Enhanced SERS Hot Spots in Protein Microarray Analysis. *Anal Chem* 84(21): 9139-9145.
67. Li M, Cushing SK, Zhang J, Suri S, Evans R, et al. (2013) Three-Dimensional Hierarchical Plasmonic Nano-Architecture Enhanced Surface-Enhanced Raman Scattering Immunosensor for Cancer Biomarker Detection in Blood Plasma. *ACS Nano* 7(6): 4967-4976.
68. Luo Z, Li W, Lu D, Chen K, He Q, et al. (2013) A SERS-based immunoassay for porcine circovirus type 2 using multi-branched gold nanoparticles *Microchim Acta* 180(15-16): 1501-1507.
69. Tang J, Sun J, Lui R, Zhang Z, Liu J, et al. (2016) New Surface-Enhanced Raman Sensing Chip Designed for On-Site Detection of Active Ricin in Complex Matrices Based on Specific Depurination. *ACS Appl Mater Interfaces* 8(3): 2449-2455.
70. Qian XM, Peng XH, Ansari DO, Yin-Goen Q, Chen GZ, et al. (2008) *In vivo* tumor targeting and spectroscopic detection with surface-enhanced Raman nanoparticle tags. *Nat Biotechnol* 26: 83-90.
71. Lim DK, Jeon KS, Kim HM, Nam JM, Suh YD (2010) Nanogap-engineered Raman-active nanodumbbells for single-molecule detection. *Nat Mater* 9: 60-67.
72. Wang Y, Zhang CH, Tang LJ, Jiang JH (2012) Enzymatic Control of Plasmonic Coupling and Surface Enhanced Raman Scattering Transduction for Sensitive Detection of DNA Demethylation *Anal Chem* 84(20): 860-8606.
73. Seydack M (2005) Nanoparticle labels in immunosensing using optical detection methods. *Biosens Bioelectron* 20(12): 2454-2469.
74. Chen K, Han H, Luo Z, Wang Y, Wang X (2012) A Practicable Detection System for Genetically Modified Rice by SERS-barcode Nanosensors. *Biosens Bioelectron* 34(1): 118-124.
75. Ye S, Wu Y, Zhai X, Tang B (2015) Asymmetric Signal Amplification for Simultaneous SERS Detection of Multiple Cancer Markers with Significantly Different Levels. *Anal Chem* 87(16): 8242-8249.
76. Wen CY, Wu LL, Zhang ZL, Liu YL, Wei SZ, et al. (2014) Quick-Response Magnetic Nanospheres for Rapid, Efficient Capture and Sensitive Detection of Circulating Tumor Cells. *ACS Nano* 8(1): 941-949.
77. Wang X, Qian XM, Beitler JJ, Chen ZG, Khuri FR, et al. (2011) Detection of Circulating Tumor Cells in Human Peripheral Blood using Surface-Enhanced Raman Scattering Nanoparticles. *Cancer Res* 71(5): 1526-1532.
78. Wu X, Luo L, Yang S, Ma X, Li Y, et al. (2015) Improved SERS Nanoparticles for Direct Detection of Circulating Tumor Cells in the Blood. *ACS Appl Mater Interfaces* 7(18): 9965-9971.
79. Dudak FC, Boyacı IH (2009) Rapid and label-free bacteria detection by surface plasmon resonance (SPR) biosensors. *Biotechnol J* 4(7): 1003-1011.
80. Ashley J, Li SFY (2013) An aptamer based surface plasmon resonance biosensor for the detection of bovine catalase in milk. *Biosens Bioelectron* 48: 126-131.
81. McPhillips J, Murphy JA, Jonsson MP, Hendren WR, Atkinson R, et al. (2010) High-Performance Biosensing Using Arrays of Plasmonic Nanotubes. *ACS Nano* 4(4): 2210-2216.
82. Sim HR, Wark AW, Lee HJ (2010) Attomolar Detection of Protein Biomarkers Using Biofunctionalized Gold Nanorods With Surface Plasmon Resonance. *Analyst* 135(10): 2528-2532.
83. Shankaran DR, Gobi KVA, Miura N (2007) Recent advancements in surface plasmon resonance immunosensors detection of small molecules of biomedical, food and environment interest. *Sens Actuators B Chem* 121(1): 158-177.

84. Fernandez F, Sanchez-Baeza F, Marco MP (2012) Nanogold Probe Enhanced Surface Plasmon Resonance Immunosensor for Improved Detection of Antibiotic Residues. *Biosens Bioelectron* 34(1): 151-158.
85. Jung J, Na K, Lee J, Kimb KW, Hyun J (2009) Enhanced surface plasmon resonance by Au nanoparticles immobilized on a dielectric SiO<sub>2</sub> layer on a gold surface. *Anal Chim Acta* 651(1): 91-97.
86. Ko S, Park TJ, Kim HS, Kim JH, Cho YJ (2009) Directed self-assembly of gold binding polypeptide-protein A fusion proteins for development of gold-nanoparticle-based SPR immunosensors. *Biosens Bioelectron* 24(18): 2592-2597.
87. Wang JL, Munir A, Li ZH, Zhou HS (2009) Aptamer-Au NPs conjugates-enhanced SPR sensing for the ultrasensitive sandwich immunoassay. *Biosens Bioelectron* 25(1): 124-129.
88. Liu X, Li RZ, Li L, Li WJ, Zhou CJ (2013) *Chem J Chin Univ* 34: 1333-1338.
89. Law WC, Yong KT, Baev A, Prasad PN (2011) Sensitivity Improved Surface Plasmon Resonance Biosensor for Cancer Biomarker Detection Based on Plasmonic Enhancement. *ACS Nano* 5(6): 4858-4864.
90. Xiang Y, Zhu X, Huang Q, Zheng J, Fu W (2015) Real-Time Monitoring of Mycobacterium Genomic DNA With Target-Primed Rolling Circle Amplification by a Au Nanoparticle-Embedded SPR Biosensor. *Biosens Bioelectron* 66: 512-519.
91. Li XS, Cai WW, An JH, Kim S, Nah J, et al. (2009) Large-area synthesis of high-quality and uniform graphene films on copper foils. *Science* 324(5932): 1312-1314.
92. Shang JZ, Ma L, Li JW, Ai W, Yu T, et al. (2012) The Origin of Fluorescence from Graphene Oxide. *Gurzadyan Sci Rep* 2: 792-799.
93. Zhang J, Sun Y, Wu Q, Zhang H, Bai Y, et al. (2013) A protein A modified Au-graphene oxide composite as an enhanced sensing platform for SPR-based immunoassay. *Analyst* 138: 7175-7181.
94. Xie C, Li H, Li S, Wu J, Zhang Z (2010) Surface Molecular Self-Assembly for Organophosphate Pesticide Imprinting in Electropolymerized Poly(*p*-aminothiophenol) Membranes on a Gold Nanoparticle Modified Glassy Carbon Electrode. *Anal Chem* 82(1): 241-249.
95. Yu D, Zeng Y, Qi Y, Zhou T, Shi G (2012) A Novel Electrochemical Sensor for Determination of Dopamine Based on AuNPs@SiO<sub>2</sub> Core-Shell Imprinted Composite. *Biosens Bioelectron* 38(1): 270-277.
96. Xue C, Han Q, Wang Y, Wu J, Wen T, et al. (2013) Amperometric detection of dopamine in human serum by electrochemical sensor based on gold nanoparticles doped molecularly imprinted polymers. *Biosens Bioelectron* 49: 199-203.
97. Sun XL, Zhang LJ, Zhang HX, Qian H, Zhang YZ, et al. (2014) Development and Application of 3-Chloro-1,2-propandiol Electrochemical Sensor Based on a Polyaminothiophenol Modified Molecularly Imprinted Film. *J Agric Food Chem* 62(20): 4552-4557.
98. Shen L, Chen Z, Li YH, He SL, Xie SB, et al. (2008) Electrochemical DNAzyme Sensor for Lead Based on Amplification of DNA-Au Bio-Bar Codes. *Anal Chem* 80(16): 6323-6328.
99. Tang SR, Tong P, Lu W, Chen JF, Yan ZM, et al. (2014) A novel label-free electrochemical sensor for Hg<sup>2+</sup> based on the catalytic formation of metal nanoparticle. *Biosens Bioelectron* 59: 1-5.
100. Wang N, Lin M, Dai H, Ma H (2016) *Biosens Bioelectron* 79: 320-326.
101. Wang S, Wang Y, Zhou L, Li J, Wang S, et al. (2014) *Electrochim Acta* 132: 7-14.
102. Yang Y, Zhang S, Kang M, He L, Zhao J, et al. (2015) *Anal Biochem* Selective detection of silver ions using mushroom-like polyaniline and gold nanoparticle nanocomposite-based electrochemical DNA sensor. 490: 7-13.
103. He X, Su J, Wang Y, Wang K, Ni X, et al. (2011) *Biosens Bioelectron* 28: 298-303.
104. Wang Q, Gao F, Ni J, Liao X, Zhang X, et al. (2016) Facile construction of a highly sensitive DNA biosensor by *in-situ* assembly of electroactive tags on hairpin-structured probe fragment. *Sci Rep* 6: 22441.
105. Zhu D, Yan Y, Lei P, Shen B, Cheng W, et al. (2014) A novel electrochemical sensing strategy for rapid and ultrasensitive detection of Salmonella by rolling circle amplification and DNA-AuNPs probe. *Anal Chim Acta* 846: 44-50.
106. Song W, Li DW, Li YT, Li Y, Long YT (2011) Disposable biosensor based on graphene oxide conjugated with tyrosinase assembled gold nanoparticles. *Biosens Bioelectron* 26(7): 3181-3186.
107. Li C, Wei L, Liu X, Lei L, Li G (2014) *Anal Chim Acta* 831: 60e64.
108. Myung S, Park J, Lee H, Kim KS, Hong S, et al. (2010) Ambipolar Memory Devices Based on Reduced Graphene Oxide and Nanoparticles. *Adv Mater* 22(18): 2045-2049.
109. Huang KJ, Niu DJ, Liu X, Wu ZW, Fan Y, et al. (2011) "Direct Electrochemistry of Catalase at Amine-Functionalized Graphene/Gold Nanoparticles Composite Film for Hydrogen Peroxide Sensor. *Electrochim Acta* 56(7): 2947-2953.
110. Cui P, Seo S, Lee J, Wang L, Lee E, Min M, et al. (2011) Nonvolatile Memory Device Using Gold Nanoparticles Covalently Bound to Reduced Graphene Oxide. *ACS Nano* 5(9): 6826-6833.
111. Zheng J, He Y, Sheng Q, Zhang H (2011) DNA as a linker for biocatalytic deposition of Au nanoparticles on graphene and its application in glucose detection. *J Mater Chem* 21: 12873-12879.
112. Liu J, Fu S, Yuan B, Li Y, Deng Z (2010) Toward a Universal "Adhesive Nanosheet" for the Assembly of Multiple Nanoparticles Based on a Protein-Induced Reduction/Decoration of Graphene Oxide. *J Am Chem Soc* 132(21): 7279-7281.
113. Liu G, Qi M, Zhang Y, Cao C, Goldys EM (2016) Nanocomposites of gold nanoparticles and graphene oxide towards a stable label-free electrochemical immunosensor for detection of cardiac marker troponin-I. *Anal Chim Acta* 909: 1-8.
114. Karaboga MNS, Simsek CS, Sezgin MK (2016) *Biosens Bioelectron* 84: 22-29.
115. Wang L, Hua E, Liang M, Ma C, Liu Z, et al. (2014) Graphene sheets, polyaniline and AuNPs based DNA sensor for electrochemical determination of BCR/ABL fusion gene with functional hairpin probe. *Biosens Bioelectron* 51: 201-207.
116. Su S, Zou M, Zhao H, Yuan C, Xu Y, et al. (2015) Shape-controlled gold nanoparticles supported on MoS<sub>2</sub> nanosheets: synergistic effect of thionine and MoS<sub>2</sub> and their application for electrochemical label-free immunosensing. *Nanoscale* 7: 19129-19135.



117. Su S, Sun H, Cao W, Chao J, Peng H, et al. (2016) Dual-Target Electrochemical Biosensing Based on DNA Structural Switching on Gold Nanoparticle-Decorated MoS<sub>2</sub> Nanosheets. *ACS Appl Mater Interfaces* 8(11): 6826-6833.
118. Das J, Kelley SO (2011) Protein Detection Using Arrayed Microsensor Chips: Tuning Sensor Footprint to Achieve Ultrasensitive Readout of CA-125 in Serum and Whole Blood. *Anal Chem* 83(4): 1167-1172.
119. Johari-Ahar, Rashidi MR, Barar J, AghaieaM, MohammadnejadaD (2015) An ultra-sensitive impedimetric immunosensor for detection of the serum oncomarker CA-125 in ovarian cancer patients. *Nanoscale* 7: 3768-3779.
120. Serafin V, Martinez-Garcia G, Agui L, Ynez-Sedeno P, Pingarron JM (2014) Multiplexed determination of human growth hormone and prolactin at a label free electrochemical immunosensor using dual carbon nanotube–screen printed electrodes modified with gold and PEDOT nanoparticles. *Analyst* 139: 4556-4563.
121. Cui H, Xu Y, Zhang ZF (2004) Multichannel Electrochemiluminescence of Luminol in Neutral and Alkaline Aqueous Solutions on a Gold Nanoparticle Self-Assembled Electrode. *Anal Chem* 76(14): 4002-4010.
122. Li M, Zhang M, Ge S, Yan M, Yu J, et al. (2013) *Sens Actuators B* 181: 50-56.
123. Cao Y, Yuan R, Chai Y, Mao L, Niu H, et al. (2012) Ultrasensitive Luminol Electrochemiluminescence for Protein Detection Based on in Situ Generated Hydrogen Peroxide as Coreactant With Glucose Oxidase Anchored AuNPs@MWCNTs Labeling. *Biosens Bioelectron* 31(1): 305-309.
124. Gui GF, Zhuo Y, Chai YQ, Xiang Y, Yuan R (2015) *Biosens Bioelectron* 70: 221-225.
125. Wang J, Shan Y, Zhao WW, Xu JJ, Chen HY (2011) Gold Nanoparticle Enhanced Electrochemiluminescence of CdS Thin Films for Ultrasensitive Thrombin Detection. *Anal Chem* 83(11): 4004-4011.
126. Wang D, Guo L, Huang R, Qiu B, Lin Z, et al. (2015) Surface Enhanced Electrochemiluminescence of Ru(bpy)<sub>3</sub><sup>2+</sup>. *Sci Rep* 5: 7954.
127. Wang D, Guo L, Huang R, Qiu B, Lin Z, et al. (2014) *Electrochim Acta* 150: 123-128.
128. Wang D, Li Y, Lin Z, Qiu B, Guo L (2015) Surface-Enhanced Electrochemiluminescence of Ru@SiO<sub>2</sub> for **Ultrasensitive Detection of Carcinoembryonic Antigen**. *Anal Chem* 87(12): 5966-5972.
129. Kerman K, Vestergaard MD, Tamiya E (2007) Label-Free Electrical Sensing of Small-Molecule Inhibition on Tyrosine Phosphorylation. *Anal Chem* 79(17): 6881-6885.
130. Wilkins MHF, Stokes AR, Wilson HR (1953) Molecular Structure of Deoxyribose Nucleic Acids. *Nature* 171: 738-740.
131. Sessler JL, Lawrence CM, Jayawickramarajah (2007) Molecular recognition *via* **base-pairing**. *J Chem Soc Rev* 36: 314-325.
132. Kerman K, Chikae M, Yamamura S, Tamiya E (2007) Gold nanoparticle-based electrochemical detection of protein phosphorylation. *Anal Chim Acta* 588(1): 26-33.
133. Xu X, Nie Z, Chen J, Fu Y, Li W, et al. (2009) *Chem Commun* 694: 6-6948.
134. Wang Z, Sun N, He Y, Liu Y, Li J (2014) DNA Assembled Gold Nanoparticles Polymeric Network Blocks Modular Highly Sensitive Electrochemical Biosensors for Protein Kinase Activity Analysis and Inhibition. *Anal Chem* 86(12): 6153-6159.
135. Jing X, Cao X, Wang L, Lan T, Li Y, et al. (2014) DNA-AuNPs based signal amplification for highly sensitive detection of DNA methylation, methyltransferase activity and inhibitor screening. *Biosens Bioelectron* 58: 40-47.
136. Liang H, Zhang XB, Lv Y, Gong L, Wang R, et al. (2014) Functional DNA-Containing Nanomaterials: Cellular Applications in Biosensing, Imaging, and Targeted Therapy. *Acc Chem Res* 47(6): 1891-1901.
137. Lee DE, Koo H, Sun IC, Ryu JH, Kim K, et al. (2012) Multifunctional nanoparticles for multimodal imaging and theragnosis. *Chem Soc Rev* 41: 2656-2672.
138. Li Z, Cheng E, Huang W, Zhang T, Yang Z, et al. (2011) Improving the Yield of Mono-DNA-Functionalized Gold Nanoparticles through Dual Steric Hindrance. *Am Chem Soc* 133(39): 15284-15287.
139. Hallouard N, Anton P, Choquet A, Constantinesco T, Vandamme (2010) Iodinated blood pool contrast media for preclinical X-ray imaging applications – a review. *Biomaterials* 31(24): 6249-6268.
140. Kim D, Park S, Lee JH, Jeong YY, Jon S (2007) Antibiofouling Polymer-Coated Gold Nanoparticles as a Contrast Agent for in Vivo X-ray Computed Tomography Imaging. *J Am Chem Soc* 129(24): 7661-7665.
141. Liu Y, Ai K, Liu J, Yuan Q, He Y, et al. (2011) A High-Performance Ytterbium-Based Nanoparticulate Contrast Agent for in Vivo X-Ray Computed Tomography Imaging. *Chem Int Ed* 51(6): 1437-1442.
142. McQuaid HN, Muir MF, Taggart LE, McMahon SJ, Coulter JA, et al. (2016) Imaging and radiation effects of gold nanoparticles in tumour cells. *Sci Rep* 6: 19442.
143. Hainfeld JF, Smilowitz DN, Slatkin HM (2004) The use of gold nanoparticles to enhance radiotherapy in mice. *Phys Med Biol* 49(18): N309-N315.
144. Peng C, Wang H, Guo R, Shen MW, Cao XY, et al. (2011) Acetylation of Dendrimer-Entrapped Gold Nanoparticles: Synthesis, Stability, and X-ray Attenuation Properties. *J Appl Polym Sci* 119(3): 1673-1682.
145. Peng C, Zheng L, Chen Q, Shen M, Guo R (2011) et al. PEGylated Dendrimer-Entrapped Gold Nanoparticles for in Vivo Blood Pool and Tumor Imaging by Computed Tomography. *Biomaterials* 33(4): 1107-1119.
146. Peng C, Li K, Cao X, Xiao T, Hou W, et al. (2012) Facile formation of dendrimer-stabilized gold nanoparticles modified with diatrizoic acid for enhanced computed tomography imaging applications. *Nanoscale* 4: 6768-6778.
147. Li C, Chen T, Ochoy I, Zhu G, Yasun E, et al. (2014) Gold-Coated Fe<sub>3</sub>O<sub>4</sub> Nanoroses with Five Unique Functions for Cancer Cell Targeting, Imaging and Therapy. *Adv Funct Mater* 24(12): 1772-1780.
148. Zhang Y, Wen S, Zhao L, Li D, Liu C, et al. (2015) Ultrasensitive polyethyleneimine-stabilized gold nanoparticles modified with polyethylene glycol for blood pool, lymph node and tumor CT imaging. *Nanoscale* 8: 5567-5577.

149. Wen S, Li K, Cai H, Chen Q, Shen M, et al. (2013) Multi-functional dendrimer- entrapped gold nanoparticles for dual mode CT/ MR imaging applications. *Biomaterials* 34(5): 1570-1580.
150. Zhang XD, Chen J, Luo Z, Wu D, Shen X, et al. (2014) Enhanced tumor accumulation of sub-2 nm gold nanoclusters for cancer radiation therapy. *Adv Healthcare Mater.* *Adv Healthcare Mater* 3(1): 133-141.
151. Huang P, Bao L, Zhang C, Lin J, Luo T, et al. (2011) Folic acid-conjugated silica-modified gold nanorods for X-ray/CT imaging-guided dual-mode radiation and photo-thermal therapy. *Biomaterials* 32(36): 9796-9809.
152. Lee N, Choi SH, Hyeon T(2013) Nano-Sized CT Contrast Agents. *Adv Mater* 25(19): 2641-2660.
153. Dou Y, Guo Y, Li X, Li X, Wang S, et al. (2016) Size-Tuning Ionization To Optimize Gold Nanoparticles for Simultaneous Enhanced CT Imaging and Radiotherapy. *ACS Nano* 10: 2536-2548.
154. Hainfeld JF, Slatkin DN, Focella TM, Smilowitz HM (2006) Gold nanoparticles: a new X-ray contrast agent. *J Radiol* 79(939): 248-253.
155. Rand D, Oritz V, Liu Y, Derdak Z, Wands JR, et al. (2011) Nanomaterials for X-ray Imaging: Gold Nanoparticle Enhancement of X-ray Scatter Imaging of Hepatocellular Carcinoma. *Nano Lett* 11(7): 2678-2683.
156. ChienCC, Chen HH, Lai SF, Wu KC, Cai X, et al. (2012) *J Nanobiotechnol* 10: 10-21.
157. KimCK, Ghosh P, Rotello V(2009)*Nanoscale* 1: 61-68.
158. Giljohann DA, Seferos DS, Daniel WL, Massich MD, Patel PC, et al. (2010) Gold nanoparticles for biology and medicine. *ChemInt Ed* 49(19): 3280-3294.
159. Lin J, Zhang H, Chen Z, Zheng Y(2010) Penetration of Lipid Membranes by Gold Nanoparticles: Insights into Cellular Uptake, Cytotoxicity, and Their Relationship. *ACS Nano* 4(9): 5421-5429.
160. Oh E, Delehanty J, Sapsford K, Susumu K, Goswami R, et al. (2011) Cellular Uptake and Fate of PEGylated Gold Nanoparticles Is Dependent on Both Cell-Penetration Peptides and Particle Size. *ACS Nano* 5(8): 6434-6448.
161. Bartczak D, Nitti S, Millar TM, Kanaras AG (2012) Exocytosis of peptide functionalized gold nanoparticles in endothelial cells. *Nanoscale* 4: 4470-4472.
162. Marchesano V, Hernandez Y, Salvenmoser W, Ambrosone A, Tino A, et al. (2013) Imaging Inward and Outward Trafficking of Gold Nanoparticles in Whole Animals. *ACS Nano* 7(3): 2431-2442.
163. Yigit MV, Zhu L, Ifediba MA, Zhang Y, Carr K, et al. (2011) Noninvasive MRI-SERS Imaging in Living Mice Using an Innately Bimodal Nanomaterial. *ACS Nano* 5(2): 1056-1066.
164. Kong KV, Lam Z, Goh WD, Leong WK, Olivo M(2012) Metal carbonyl-gold nanoparticle conjugates for live-cell SERS imaging. *ChemInt Ed* 51(39): 9796-9799.
165. Wang Y, Black KCL, Luehmann H, Li W, Zhang Y, et al. (2013) Comparison Study of Gold Nanohexapods, Nanorods, and Nanocages for Photothermal Cancer Treatment. *ACS Nano* 7(3): 2068-2077.
166. Kircher MF, de la Zerda A, Jokerst JV, Zavaleta CL, Kempen PJ, et al. (2012) A brain tumor molecular imaging strategy using a new triple-modality MRI-photoacoustic-Raman nanoparticle. *Nat Med* 18: 829-834.
167. Zavaleta CL, Garai E, Liu JTC, Sensarn S, Mandella MJ, et al. (2013) A Raman-based endoscopic strategy for multiplexed molecular imaging. *ProcNatlAcadSci USA* 110(25): E2288-E2297.
168. Oh JW, Lim DK, Kim GH, Suh YD, Nam JM (2014) Thiolated DNA-Based Chemistry and Control in the Structure and Optical Properties of Plasmonic Nanoparticles with Ultrasmall Interior Nanogap. *J Am ChemSoc* 136(40): 14052-14059.
169. Tian L, Tadepalli S, Fei M, Morrissey JJ, Kharasch ED, et al. (2015) Off-Resonant Gold Superstructures as Ultrabright Minimally Invasive Surface-Enhanced Raman Scattering (SERS) Probes. *Chem Mater* 27(16): 5678-5684.
170. Srivastava S, Santos A, Critchley K, Kim KS, Podsiadlo P, et al. (2010) Light-controlled self-assembly of semiconductor nanoparticles into twisted ribbons. *Science* 327(5971): 1355-1359.
171. Peilong Wang, Zhenyu Lin, Xiaouu Su, Zhiyong Tang (2017) Application of Au based nanomaterials in analytical science. *Nano Today* 12: 64-97.
172. Wu DY, Li JF, Ren B, Tian ZQ (2008) Electrochemical surface-enhanced Raman spectroscopy of nanostructures. *Chem Soc Rev* 37: 1025-1041.
173. Shang L, Dong SJ, Ulrich Nienhaus G (2011) Ultra-small fluorescent metal nanoclusters: synthesis and biological applications. *Nano Today* 6(4): 401-418.